NATIONAL ADVISORY COMMITTEE FOR AERONAUTICS

TECHNICAL NOTE 3663

DISCHARGE COEFFICIENTS FOR COMBUSTOR-LINER AIR-ENTRY HOLES

I - CIRCULAR HOLES WITH PARALLEL FLOW

By Ralph T. Dittrich and Charles C. Graves

Lewis Flight Propulsion Laboratory
Cleveland, Ohio

Washington
April 1956

NATIONAL ADVISORY COMMITTEE FOR AERONAUTICS

TECHNICAL NOTE 3663

DISCHARGE COEFFICIENTS FOR COMBUSTOR-LINER AIR-ENTRY HOLES

I - CIRCULAR HOLES WITH PARALLEL FLOW

By Ralph T. Dittrich and Charles C. Graves

SUMMARY

An experimental investigation was conducted to determine the effects of various geometric and flow factors on the discharge coefficients for circular holes having flow parallel to the plane of the hole. The geometric and flow factors considered were hole diameter, wall thickness at the hole, parallel-flow duct height, boundary-layer thickness, parallel-flow velocity, static-pressure level, and pressure ratio across the test hole.

Discharge coefficients, corrected for pressure-ratio effects, were correlated with a flow parameter incorporating the total and static pressures of the discharge jet and of the parallel-flow stream. Within the range investigated, the effects of hole diameter and wall thickness at the hole on discharge coefficients were small compared with the effects of parallel-flow velocity and static-pressure ratio across the hole. The effects of duct height, boundary-layer thickness, and static-pressure level were negligible.

INTRODUCTION

Knowledge of the discharge coefficients of combustor-liner wall openings is essential in the calculation of total-pressure loss and liner air-flow distribution for turbojet and can-type ram-jet combustors. Accordingly, one phase of a research program being conducted at the NACA Lewis laboratory on combustors is concerned with the determination of the discharge coefficients of these openings. This report covers an investigation of the discharge coefficients for circular holes.

The discharge coefficient of a square-edged, thin-plate orifice, where the flow is normal to the plane of the orifice, is a function of the geometry of the flow passage and orifice as well as the flow conditions (ref. 1). Geometric factors include orifice diameter and thickness as well as duct diameter and straight length; flow factors include Reynolds and Mach numbers. For air admission holes in typical combustor

liners, however, the flows in the passage outside the liner (external flow) and inside the liner (internal flow) are essentially parallel to the plane of the opening. Under these conditions, additional geometric and flow factors must be considered. These include (1) the geometry of the hole relative to that of the external- and internal-flow passages, (2) the external and internal velocities relative to the jet velocity, (3) the external- and internal-flow densities, and (4) the external- and internal-velocity profiles (refs. 2 to 6).

Previous investigations (refs. 2 to 6) of the discharge coefficients for holes with parallel flow have been confined to the study of the effects of flow velocities and hole diameter and were limited in range of operational variables. In these investigations, it was found that hole discharge coefficients vary appreciably with both internal and external parallel flow. However, for a complete analysis of combustor aerodynamics, the effect of the various other geometric and flow factors on the discharge coefficient of liner wall openings must also be known.

This investigation supplements existing data for the discharge coefficient of circular holes with parallel flow. The geometric and flow factors studied, with their ranges, are as follows: (1) hole diameter, 0.125 to 1.50 inches, (2) external-flow passage height, 0.74 to 2.23 inches, (3) wall thickness at hole, 0.040 to 0.500 inch, (4) external-parallel-flow velocity, 0 to 500 feet per second, (5) static-pressure drop across test hole, 1.0 to 470 pounds per square foot, (6) boundary-layer thickness of external-parallel-flow stream, 0.040 to 0.100 inch, and (7) static pressure of external stream, 1060 to 3605 pounds per square foot absolute. The airstream temperature was approximately 75° F. For the present tests the internal parallel flow was zero. The results of references 2 and 4 indicate that the data should be applicable to the case of combined internal and external parallel flow provided the jet velocity is greater than the internal-parallel-flow velocity and the correct jet-outlet static pressure is used.

The data are correlated on the basis of flow parameters and show the magnitude of the effect of the geometric factors on the discharge coefficients of circular holes.

SYMBOLS

The following symbols are used in this report:

A_d area of duct cross section, sq ft

A_h area of circular hole, sq ft

C	discharge coefficient, ratio of measured to theoretical flow through hole
C_p	discharge coefficient, corrected for pressure ratio effect
$C_{p,a}$	discharge coefficient, corrected for pressure ratio effect, for a given wall thickness
$C_{p,b}$	discharge coefficient, corrected for pressure ratio effect, for a 0.040-inch-thick wall
$C_{p,t}$	discharge coefficient, corrected for pressure ratio and wall thickness effects
c_p	specific heat of air at constant pressure, 0.24 Btu/lb/^{o}R
g	acceleration due to gravity, 32.2 ft/sec^2
J	mechanical equivalent of heat, 778 ft-lbs/Btu
P_d	total pressure of duct air, lb/sq ft abs
p_d	static pressure of duct air, lb/sq ft abs
p_j	static pressure of jet air, lb/sq ft abs
T_d	total or stagnation temperature of duct air, ^{o}R
V_d	velocity of approach stream at hole in duct, ft/sec
V_j	velocity of jet, ft/sec
w_{th}	theoretical mass flow of air through hole, lb/sec
w_h	measured mass flow of air through hole, lb/sec
ρ_d	mass density of air at duct static pressure and temperature, slugs/cu ft
ρ'_d	mass density of air at duct total pressure and temperature, slugs/cu ft
ρ_j	mass density of air at jet static pressure and temperature, slugs/cu ft

APPARATUS

Test Section

A sketch of the apparatus used for the study of discharge coefficients for circular holes having external parallel flow is shown in figure 1. The inlet of the 4-inch square duct was connected to either the laboratory air-supply system or room air, and the outlet was connected to the laboratory low-pressure exhaust system. The duct static pressure and air-flow rate were controlled by means of valves located upstream and downstream of the test section. Methods for varying test-hole diameter, test-plate thickness, duct height, and boundary-layer thickness were incorporated in the design of the test section. A portion (4.0 by 8.5 in.) of one wall of the test-section duct was replaced by a 0.040-inch-thick metal plate containing the square-edged test hole. The test plate was located flush with the inside of the duct wall, reinforced on the downstream side by a metal frame, and held in place and sealed along its edges by a high-temperature sealing wax. Although the face of the test plate was flat rather than curved as in combustor liners, the effect of this difference in hole geometry on the discharge coefficient for a circular hole was assumed negligible. A plenum chamber enclosing the test plate was connected to the low-pressure exhaust system through a flow control valve and an air metering system.

Four 0.040-inch-thick test plates having nominal hole diameters of 0.125, 0.25, 0.75, and 1.50 inches were used. The plates with 0.125- and 0.25-inch-diameter holes contained five holes each. These holes were spaced 1/2 inch apart, center to center, along a line normal to the duct axis. The multiple holes were used to maintain flow rates in a range of sufficient accuracy. For the larger holes (0.75- and 1.50-in. diam.), a single hole was used. Plate thickness at the 0.75-inch-diameter test hole was varied by coaxially attaching a ring of the desired thickness and having an inside diameter equal to that of the test hole to the low-pressure side of the test plate.

Duct height was varied by mounting wood blocks of the desired thickness in the duct opposite the test-plate wall (fig. 1(a)). The upstream end of the blocks (contraction section) had an elliptical profile with a major- to minor-axis ratio of 2. The distance from the downstream end of the contraction section to the center of the test hole was 2.75 inches for test holes 0.75-inch diameter and smaller. With the 1.50-inch-diameter test hole, this distance was 6.75 inches for a test with a 0.74-inch duct height and 9.75 inches for a test with a 2.23-inch duct height. A 30-mesh screen was located at the test-section upstream flange in order to provide a uniform velocity distribution.

In order to vary the boundary-layer thickness, the test apparatus was modified as shown in figure 1(b). The test plate was mounted on a

partition member and immersed 1/4 inch into the duct stream, thereby forming a boundary-layer bleedoff slot at its upstream edge. This partition member, which was sandwiched between the test section and the plenum chamber, isolated the boundary-layer bleedoff air from the test-hole air. The boundary-layer bleedoff passage was connected to the laboratory low-pressure exhaust system through a flow control valve and an air metering system.

Instrumentation

A measurement of duct pressures as close to the test hole as possible was desired because of total- and static-pressure variations along the approach duct due to wall friction and changes in velocity profile. However, preliminary pressure surveys indicated that, with a large hole and small duct-height configuration and a given duct total pressure and velocity, the static pressure at the duct wall opposite the center of the test hole varied with flow through the test hole. Therefore, total and static pressures were measured at stations located $3\frac{1}{4}$ inches upstream of the center of the 1.50-inch-diameter hole and 1 inch upstream of the test holes having diameters 0.75 inch and smaller. Pressures at these upstream stations remained constant throughout the range of test-hole air flows with all configurations investigated.

The probe used for determining duct total pressure and boundary-layer profile is shown in figure 1(a). The probe tip was made from tubing having a 0.020-inch outside diameter and a 0.002-inch wall thickness flattened to 0.010 inch and measured $4\frac{1}{16}$ inches from the probe stem axis. A traverse of a portion of the duct was possible by rotating the probe stem through a small angle. Reference 7 indicates that a thin-wall, blunt-nose total-pressure tube is insensitive to misalinement between tube and stream within the range of ±11 degrees. The probe stem was electrically insulated from the test section in order that, as the probe stem was rotated, contact of the probe tip with the duct wall could be indicated by electrical continuity. Positioning of the probe tip in the duct was controlled by a micrometer acting upon a lever which rotated the probe stem. Jet static-pressure taps were located on the downstream face of the test plate as shown in figure 1(a). The location of the jet static-pressure taps was not critical in the absence of parallel flow on the downstream face of the test plate.

PROCEDURE

Hole discharge-coefficient and boundary-layer-profile data were obtained for the following series of tests:

Number of holes	Hole diam., in.	Test-plate thickness, in.	Duct height, in.	Duct static pressure, lb/sq ft abs	Boundary-layer bleedoff
5	0.125	0.040	1.98	1910	Yes
5	.125	.040	2.23	1910	No
5	.25	.040	2.23	1910	No
5	.25	.040	1.98	1910	Yes
1	.75	.040	2.23	1910	No
1	.75	.125	2.23	1910	No
1	.75	.500	2.23	1910	No
1	.75	.040	2.23	1060	No
1	.75	.040	2.23	3605	No
1	1.50	.040	.74	1910	No
1	1.50	.040	2.23	1910	No

Each test series was run at external-parallel-flow velocities of 0, 40, 70, 150, 300, and 500 feet per second. At each velocity condition. the static-pressure difference across the test hole was varied from 1.0 to 470 pounds per square foot, when practical. The duct-air temperature was approximately 75° F for all tests.

CALCULATIONS

The discharge coefficient C was calculated as the ratio of the measured mass flow to the theoretical mass flow through the hole w_h/w_{th}. The theoretical mass flow w_{th} was calculated as the product of the jet velocity V_j, the jet density ρ_j, and the hole area A_h. Assuming isentropic flow, the jet velocity V_j and the jet density ρ_j were determined from compressible-flow relations utilizing the duct total pressure P_d and total temperature T_d and the jet static pressure p_j.

RESULTS AND DISCUSSION

The data for zero crossflow with the various hole and flow passage geometries will be presented first. Then, data for parallel flow with one geometric configuration will be considered and used to illustrate the method for correlation of the data. Finally, the correlated data for all geometric configurations and flow conditions investigated will be examined and compared.

Effects of Pressure Ratio

With zero crossflow. - Data presented in figure 2 show the variation in discharge coefficient with static-pressure ratio at zero crossflow for all hole and duct configurations tested. A hole having zero crossflow may be considered to represent the final air admission hole in a combustor liner where all the air flow approaching the hole flows through the hole. These data show that the discharge coefficient at zero crossflow varies with hole and duct geometry as well as with pressure ratio. For 0.75-inch-diameter thin-walled holes, the discharge coefficient varies from approximately 0.60 at a pressure ratio of 1.02 to approximately 0.64 at a pressure ratio of 1.30 (fig. 2). These results are comparable with those reported in reference 8 for sharp-edged orifices with normal flow. However, a decrease in hole diameter or an increase in wall thickness, so that the ratio of hole diameter to wall thickness is less than approximately 6.0 (fig. 2), tends to increase the discharge coefficient. The high discharge coefficients obtained in these cases may be the result of the relatively small diameter, long-length holes acting as short pipes (ref. 9). An effect of hole area relative to duct area on discharge coefficient is also shown in figure 2. For the configuration with a 1.50-inch-diameter hole and 0.74-inch duct height (hole-to-duct area ratio, 0.60), the discharge coefficient is appreciably less than 0.60 at a pressure ratio of 1.02. This discharge coefficient is relatively low because of an effect of approach velocity V_d which becomes appreciable for large-hole, small-duct configurations. Since, for zero crossflow, the approach velocity is related to the jet velocity by an area function $V_d = V_j \frac{\rho_j}{\rho_d} \frac{CA_h}{A_d}$, the approach velocity will approximate the jet velocity as the effective area of the hole approaches that of the duct. The important geometric factors affecting discharge coefficient at zero crossflow are the ratio of hole diameter to wall thickness and the ratio of hole area to duct area.

With parallel flow. - Discharge-coefficient data for one geometric configuration (hole diam., 0.75 in.; wall thickness, 0.040 in.; and duct height, 2.23 in.) with parallel flow are presented in figure 3. Zero crossflow data (fig. 2) for the same configuration are included to show the effect of pressure ratio alone on discharge coefficient. With this configuration, the approach velocity at zero crossflow was negligible. The data for parallel-flow velocities of 40 to 500 feet per second show the combined effect of external-parallel-flow velocity and static-pressure ratio on hole discharge coefficient. The discharge coefficient decreases with an increase in parallel-flow velocity and with a decrease in static-pressure ratio across the hole. The trends shown in this figure are typical of those observed with all configurations investigated.

Considering discharge coefficient as the ratio of jet cross-sectional area to hole area, then, for a given hole area, the discharge coefficient will be a maximum when jet area is maximum. Jet area will be a maximum when the jet axis is normal to the plane of the hole. This is the case with normal flow where the approach streamlines converge from all directions towards the center of the hole so that the discharge jet is symmetrical about the axis of the hole. With external parallel flow, however, the streamlines converge from the general direction of the approach flow so that the axis of a jet issuing from a hole in a thin plate is not normal to the plane of the hole (ref. 3). At a given parallel-flow velocity (other than zero), as the static-pressure ratio is reduced and approaches 1, the jet axis is inclined toward the wall until, in the limit, the jet axis is parallel to the wall and the jet area becomes zero. Conversely, as the pressure ratio is increased, the angle between the jet axis and the wall increases, and the discharge coefficient approaches that obtained for normal flow.

Correlation of Data

The data of figure 3 are replotted in figure 4 as a function of a dimensionless flow parameter $\frac{P_d - p_j}{P_d - p_d}$, which is the ratio of the difference between the total and static pressures of the discharge jet to the difference between the total and static pressures of the parallel-flow stream. In figure 4, the data for the various parallel-flow velocities tend to form a common curve. However, for any given parallel-flow velocity, the data fall above this common curve for the higher values of the flow parameter where the static-pressure ratio p_d/p_j is high. This increase in discharge coefficient with increases in static-pressure ratio is also indicated by the zero crossflow data of figure 3. In an attempt to determine a pressure-ratio correction factor for parallel-flow data, the zero-crossflow data of figure 3 were replotted in figure 5 as the ratio of the discharge coefficient at a given pressure ratio to the discharge coefficient at a pressure ratio of 1 (C/C_p). Discharge-coefficient data for parallel flow were then corrected for pressure-ratio effect by dividing the discharge coefficient C by a correction factor C/C_p determined from figure 5. The correlation of corrected discharge coefficient with the flow parameter for each test series is shown in figure 6.

Although the various test series had different geometric configurations, the use of pressure-ratio correction factors based on the data of figure 5 best correlated the data for all geometric configurations. Included in figure 6 are discharge coefficients for zero crossflow determined by extrapolation of the applicable faired curves in figure 2 to a pressure ratio of 1.0. These discharge coefficients were plotted

(fig. 6) at values of the flow parameter obtained from the approximate relation

$$\frac{P_d - p_j}{P_d - p_d} \approx \left(\frac{A_d}{CA_h}\right)^2$$

This relation was derived from the continuity equation assuming incompressible flow. In figures 6(a), (b), and (g) the values of these discharge coefficients for zero crossflow differ appreciably from those indicated by an extrapolation of the faired curves. This difference is due to the use of pressure-ratio correction factors based on the data of figure 5 instead of on data for like hole geometry.

Flow parameter values greater than 1 at zero discharge coefficient are indicated in figures 6(j) and (k) for 1.50-inch-diameter holes. In the case of the large hole with parallel flow but no net flow through the hole, the jet static pressure measured less than duct static pressure, which resulted in finite values of the flow parameter. Similar results are reported in reference 10 in which static-pressure measurements at a relatively large cutout of a tunnel wall, with zero net flow through the cutout, differed appreciably from tunnel-wall static pressures.

Effect of Boundary Layer

The effect of boundary layer on hole discharge coefficients was determined with test holes having 0.125- and 0.25-inch diameters. Boundary-layer thickness is defined herein as the distance from the duct wall at which the local velocity equals 0.99 of the maximum velocity. Duct velocity profiles presented in figure 7 show that boundary-layer thickness (at a plane 1 in. upstream of the center of the test hole) was reduced from approximately 0.10 inch to less than 0.04 inch by means of boundary-layer bleedoff

A comparison of the faired curves in figures 6(a), (b), (c), and (d) shows (fig. 8) that a variation in boundary-layer thickness from 0.10 to 0.04 inch has a negligible effect on the discharge coefficient for both the 0.125- and the 0.25-inch-diameter holes. A study of the duct flow indicates that, without boundary-layer bleedoff, both the average total pressure and the average velocity of the streamlines entering the test hole must be lower than those indicated by total-pressure measurements made in midstream. However, the differences in pressure and velocity may tend to compensate for each other, and the negligible effect of boundary layer shown in figure 8 may be coincidental.

Effect of Pressure Level

A comparison of faired curves for three different duct static pressures (1060, 1910, and 3605 lb/sq ft abs) shows that static-pressure level had no significant effect on the corrected discharge coefficient (fig. 9).

Effect of Wall Thickness

The effect of wall thickness on discharge coefficient for a constant-diameter hole (0.75 in.) is shown in figure 10. At values of the flow parameter less than approximately 15, an increase in wall thickness (from 0.04 to 0.50 in.) decreased the discharge coefficient; at values greater than 15, an increase in wall thickness increased the discharge coefficient. At high values of the flow parameter, where the jet velocity is large compared with approach velocity, the effect of wall thickness on discharge coefficient is similar to that shown in figure 2 for the zero-crossflow condition.

Effect of Hole Size

The faired curves from figure 6 for four different diameter holes (0.125, 0.25, 0.75, and 1.50 in.) are compared in figure 11. The corrected discharge coefficient did not vary appreciably with hole size over most of the flow range. However, at high values of the flow parameter, holes smaller than 0.75 inch in diameter had somewhat higher corrected discharge coefficients; this may not be entirely due to hole size effects. As was shown in figures 2 and 10, the discharge coefficient may be affected by wall thickness if the ratio of hole diameter to wall thickness is 6.0 or less. In the present comparison the wall thickness for all holes was 0.040 inch and the ratios of hole diameter to wall thickness for the holes with diameters of 0.125 and 0.25 inch were 3.1 and 6.2, respectively.

A comparison of corrected discharge coefficient for holes with different diameters (0.25 and 0.75 in.), but having approximately constant ratio of hole diameter to wall thickness is shown in figure 12. The hole with the smaller diameter has a somewhat larger discharge coefficient throughout the range of the flow parameter. Similar results are shown in reference 2 for the case of small holes with normal flow.

Effect of Duct Height

Figure 13 shows that with a 1.50-inch-diameter hole a decrease in duct height from 2.23 to 0.74 inches had only a small effect on the corrected discharge coefficient at low values of the flow parameter.

However, duct height, or more precisely the ratio of hole to duct areas at a station, may limit the maximum corrected discharge coefficient obtainable to values appreciably less than 0.60. With the 0.74-inch duct height (hole-to-duct area ratio, 0.60), when the flow parameter (fig. 6(j)) reached a value of 10, the mass flow through the hole equaled the mass flow approaching the hole (zero crossflow). At this value of the flow parameter, figure 6(j) shows the corrected discharge coefficient to be 0.53. Configurations having hole-to-duct area ratios greater than 0.60 would be expected to have maximum corrected discharge coefficients less than 0.53.

Corrected Discharge Coefficient

The determination of mass air flow through a given size liner hole or, conversely, of the hole size required for a given air flow requires a knowledge of the discharge coefficient for that hole. Curves of the form presented in figures 5 and 10 to 12 may be used to determine the required discharge coefficient provided the external flow is parallel to the plane of the hole (i.e., the external-flow-passage walls are parallel), and the jet velocity is greater than the internal-parallel-flow velocity. The results of references 2 and 4 indicate that discharge coefficient data for external parallel flow should be applicable to the case of combined internal and external parallel flow provided (1) the jet velocity is greater than the internal-parallel-flow velocity and (2) the correct jet-outlet static pressure is used. A method for determining discharge coefficients for liner holes is presented in the Appendix.

SUMMARY OF RESULTS

The following results were obtained from an investigation conducted to determine the effect of various geometric and flow factors on discharge coefficients for circular holes having parallel flow:

1. For each geometric configuration the discharge coefficients, corrected for pressure-ratio effects, were correlated with a flow parameter incorporating the total and static pressures of the discharge jet and of the parallel-flow stream.

2. Within the range investigated, the effects of geometric factors, such as hole size and wall thickness at the hole, on discharge coefficients for circular holes were small compared with the effects of parallel-flow velocity and static-pressure ratio across the hole. Factors such as duct height, boundary-layer thickness, and duct static-pressure level had a negligible effect on discharge coefficient.

Lewis Flight Propulsion Laboratory
National Advisory Committee for Aeronautics
Cleveland, Ohio, February 1, 1956

APPENDIX - APPLICATION OF DISCHARGE-COEFFICIENT DATA

Discharge coefficients for a given circular liner hole or hole size required for a desired air flow may be determined by the following procedures utilizing the curves of figures 5 and 10 to 12. These curves are applicable only to cases where the external flow is parallel to the plane of the hole (i.e., the external-flow passage walls are parallel). These curves may be used for the case of combined internal and external parallel flow provided the jet velocity is greater than the internal-parallel-flow velocity and the correct jet-outlet static pressure is used (refs. 2 and 4). The use of these curves requires that the total P_d and static p_d pressures of the external approach stream and the jet static pressure p_j in the liner be known. These pressures may be obtained by direct measurement in a combustor or by calculation from known values of combustor mass air flow, air density, and flow passage areas at pertinent stations.

The discharge coefficient for a given liner hole may be determined as follows:

(1) At the computed value of the flow parameter $\frac{P_d - p_j}{P_d - p_d}$, a corrected discharge coefficient C_p can be read from a curve (figs. 10 to 12) selected on the basis of geometric similarity (in diameter and wall thickness) to the given hole configuration.

(2) A pressure-ratio correction factor $\frac{C}{C_p}$ can be obtained from figure 5 at the computed value of the static-pressure ratio $\frac{p_d}{p_j}$.

(3) Then, the corrected discharge coefficient C_p (step (1)) can be multiplied by the pressure-ratio correction factor $\frac{C}{C_p}$ (step (2)) to obtain the discharge coefficient C for the hole.

The curves (figs. 5, 10 to 12) may also be used to approximate the liner hole size required for a desired mass air flow through the hole. If w_h, P_d, p_d, T_d, and p_j are known, the method is as follows:

(1) Calculate $\frac{p_d}{p_j}$, $\frac{p_j}{P_d}$, $\left(\frac{P_d - p_j}{P_d - p_d}\right)$, V_j and ρ_j. The jet velocity V_j and the jet density ρ_j may be calculated from compressible-flow

relations assuming isentropic flow as follows:

$$V_j = \sqrt{2gJc_pT_d\left[1 - \left(\frac{p_j}{P_d}\right)^{\frac{\gamma-1}{\gamma}}\right]}$$

$$\rho_j = \rho_d'\left(\frac{p_j}{P_d}\right)^{\frac{1}{\gamma}}$$

(2) Determine the effective hole area CA_h in inches squared, from the relation

$$CA_h = \frac{w_h}{\rho_j V_j}\,144$$

(3) Obtain the pressure-ratio correction factor $\frac{C}{C_p}$ from the curve in figure 5 at the calculated value of $\frac{p_d}{p_j}$.

(4) Divide CA_h (step (2)) by pressure-ratio correction factor $\frac{C}{C_p}$ (step (3)) to obtain C_pA_h.

(5) At the calculated value of the flow parameter $\left(\frac{P_d - p_j}{P_d - p_d}\right)$ a corrected discharge coefficient C_p can be read for one of the faired curves of figure 11.

(6) A first approximation of the required hole area A_h is obtained from the relation

$$A_h = \frac{(C_pA_h)}{C_p} \quad \frac{(\text{step (4)})}{(\text{step (5)})}$$

(7) If the resulting hole diameter differs appreciably from that of the faired curve used in figure 11, it may be necessary to repeat steps (5) and (6) selecting a more applicable curve in figure 11.

(8) If the given liner wall thickness differs appreciably from 0.040 inch, an estimate of the effect of wall thickness on hole discharge coefficient may be obtained from figure 10. In the use of figure 10, it is assumed that the effects of wall thickness on the discharge coefficient

may be treated in terms of the ratio of hole diameter to wall thickness, regardless of hole size. From figure 10, at the value of the flow parameter $\left(\frac{P_d - p_j}{P_d - p_d}\right)$ (from step (1)), discharge coefficients $C_{p,a}$ for the ratio of hole diameter to actual wall thickness and $C_{p,b}$ for the ratio of hole diameter to the 0.040-inch wall thickness may be determined by interpolation if necessary.

(9) Then the discharge coefficient $C_{p,t}$ corrected for wall thickness effects is obtained from

$$C_{p,t} = C_p + (C_{p,a} - C_{p,b})$$

where C_p is the value of the discharge coefficient obtained in step (5).

(10) The required hole area is then obtained from

$$A_h = \frac{(C_p A_h)}{C_{p,t}} \quad \frac{(\text{step (4)})}{(\text{step (9)})}$$

3954

REFERENCES

1. Anon.: Fluid Meters, Their Theory and Application. Fourth ed., A.S.M.E. Res. Pub., A.S.M.E. (N.Y.), 1937.

2. Callaghan, Edmund E., and Bowden, Dean T.: Investigation of Flow Coefficient of Circular, Square, and Elliptical Orifices at High Pressure Ratios. NACA TN 1947, 1949.

3. Stokes, George M., Davis, Don D., Jr., and Sellers, Thomas B.: An Experimental Study of Porosity Characteristics of Perforated Materials in Normal and Parallel Flow. NACA TN 3085, 1954. (Supersedes NACA RM L53H07.)

4. Dewey, Paul E.: A Preliminary Investigation of Aerodynamic Characteristics of Small Inclined Air Outlets at Transonic Mach Numbers. NACA TN 3442, 1955. (Supersedes NACA RM L53C10.)

5. Nelson, William J., and Dewey, Paul E.: A Transonic Investigation of the Aerodynamic Characteristics of Plate- and Bell-Type Outlets for Auxiliary Air. NACA RM L52H20, 1952.

6. Rogallo, F. M.: Internal-Flow Systems for Aircraft. NACA Rep. 713, 1941. (Supersedes NACA TN 777.)

7. Gracey, William, Letko, William, and Russel, Walter E.: Wind-Tunnel Investigation of a Number of Total-Pressure Tubes at High Angles of Attack. NACA TN 2331, 1951. (Supersedes NACA RM L50G19.)

8. Perry, J. A., Jr.: Critical Flow Through Sharp-Edged Orifices. Trans. A.S.M.E., vol. 71, Oct. 1949, pp. 757-764.

9. Schoder, Ernest W., and Davison, Francis M.: Hydraulics. Second ed., McGraw-Hill Book Co., Inc., 1934, pp. 131-133.

10. Roshko, Anatol: Some Measurements of Flow in a Rectangular Cutout. NACA TN 3488, 1955.

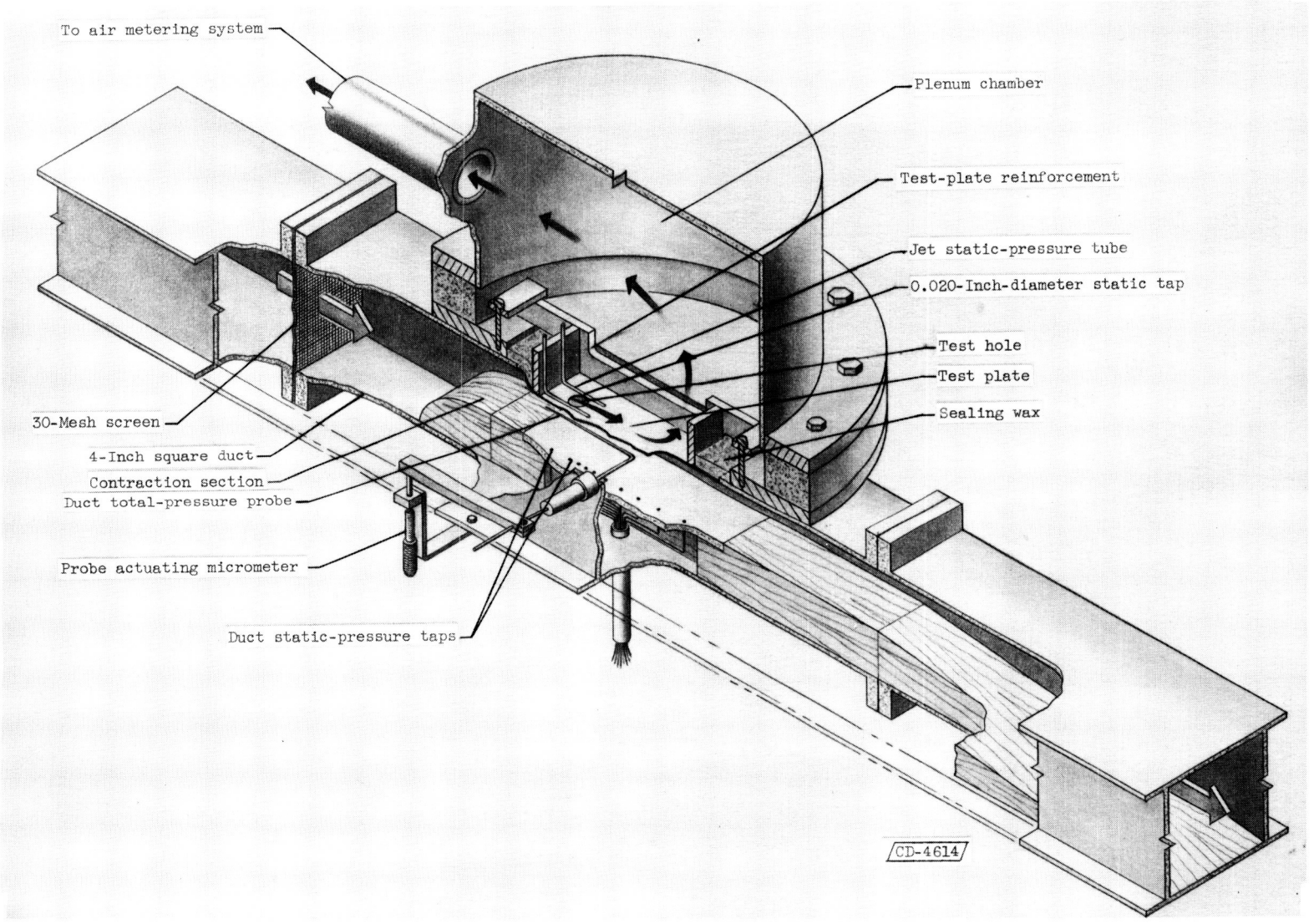

(a) Test plate flush with duct wall.

Figure 1. - Details of test apparatus for study of hole discharge coefficients.

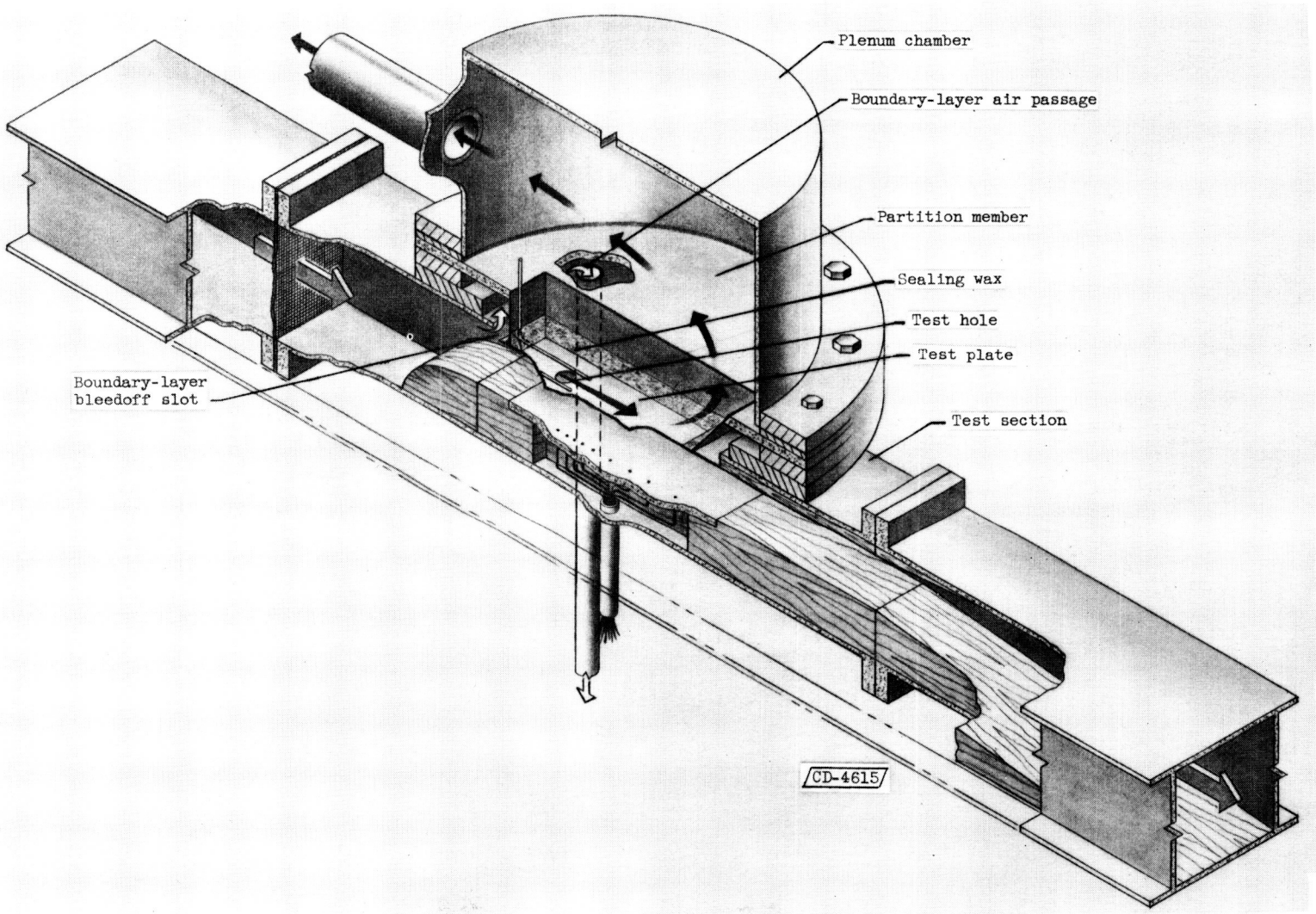

(b) Modified for boundary-layer bleedoff.

Figure 1. - Concluded. Details of test apparatus for study of hole discharge coefficients.

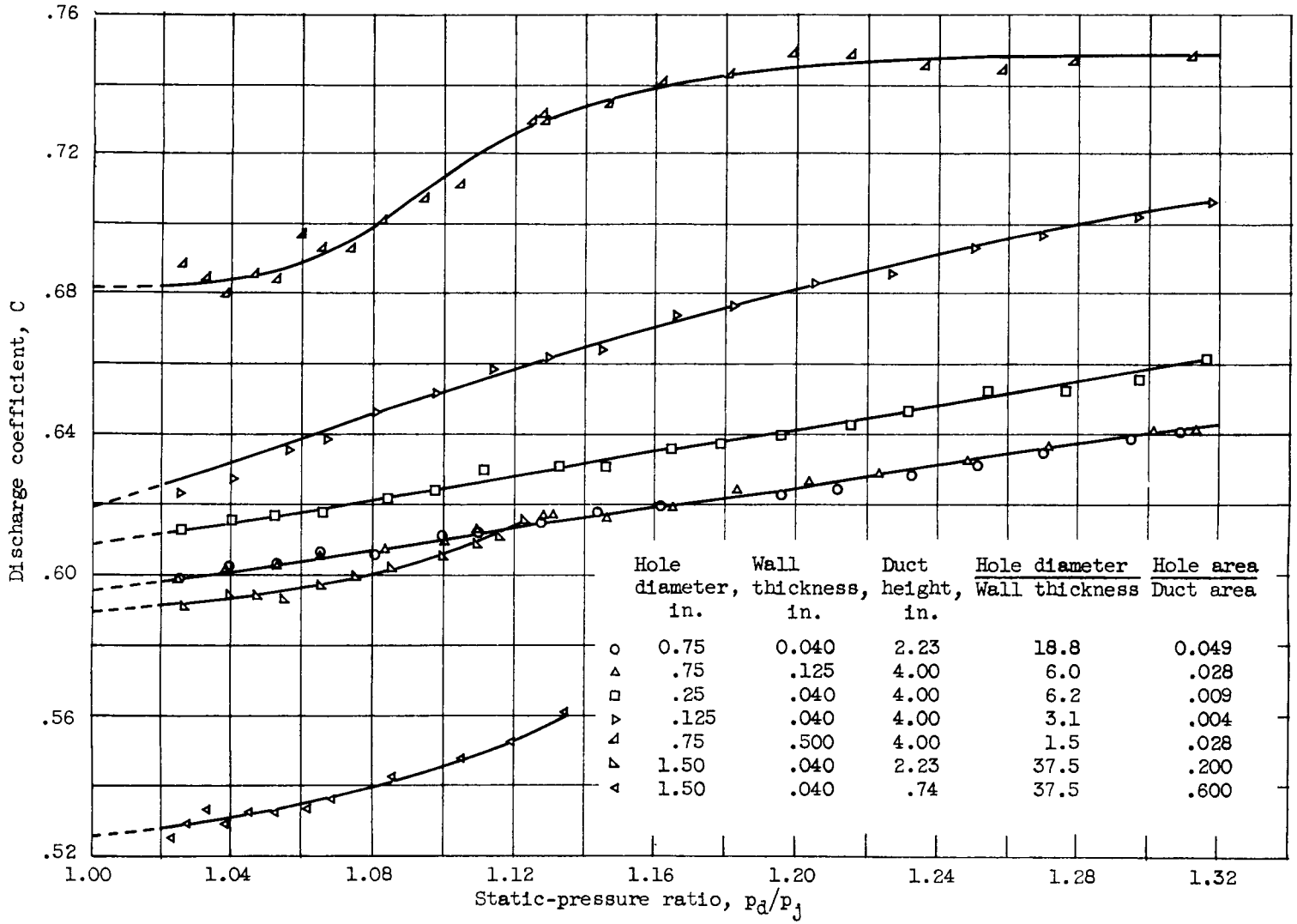

Figure 2. - Variation of hole discharge coefficient with pressure ratio for various flow passage configurations at zero crossflow.

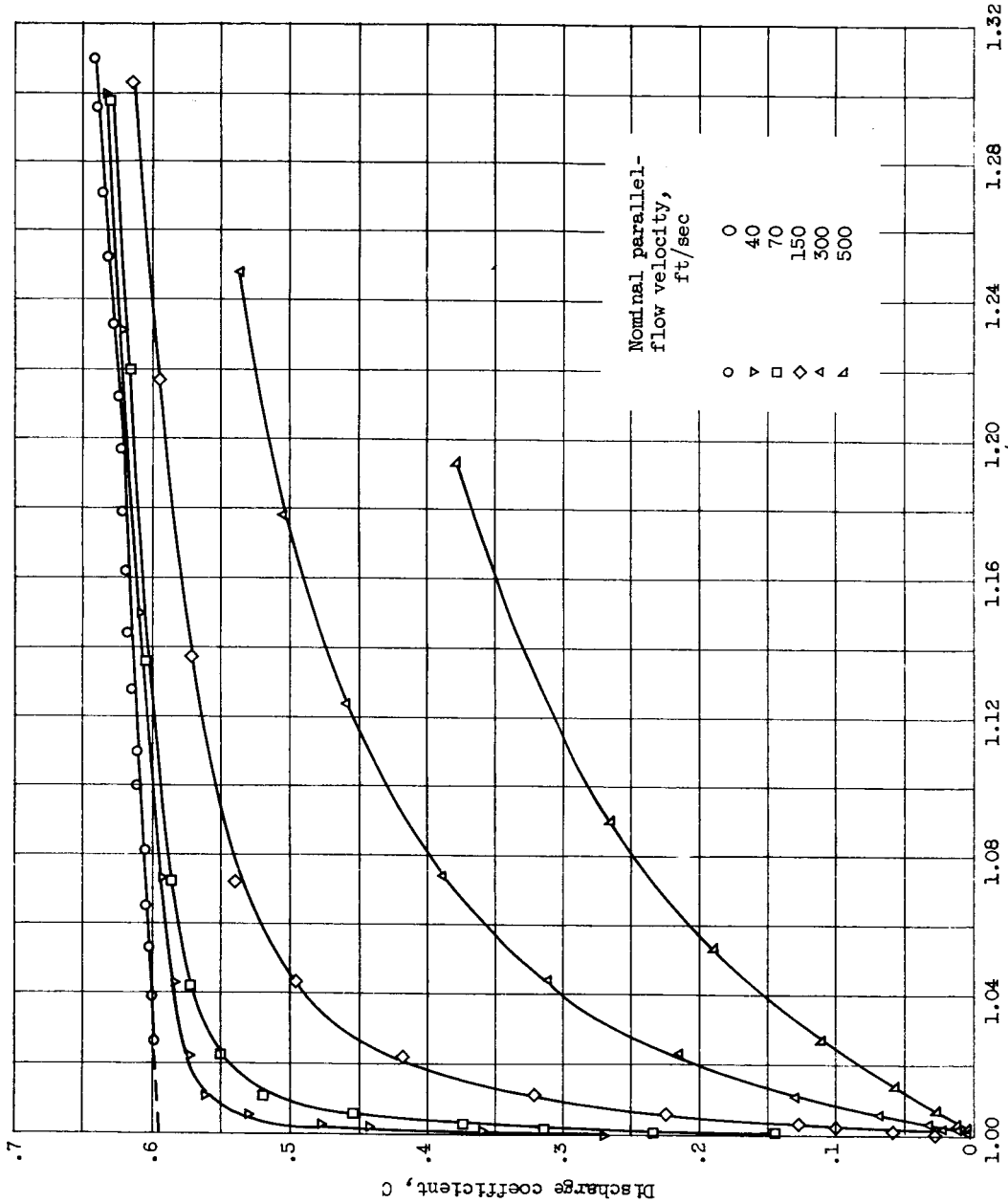

Figure 3. - Effect of static-pressure ratio on hole discharge coefficients at various parallel-flow velocities. Hole diameter, 0.75 inch; wall thickness at hole, 0.040 inch.

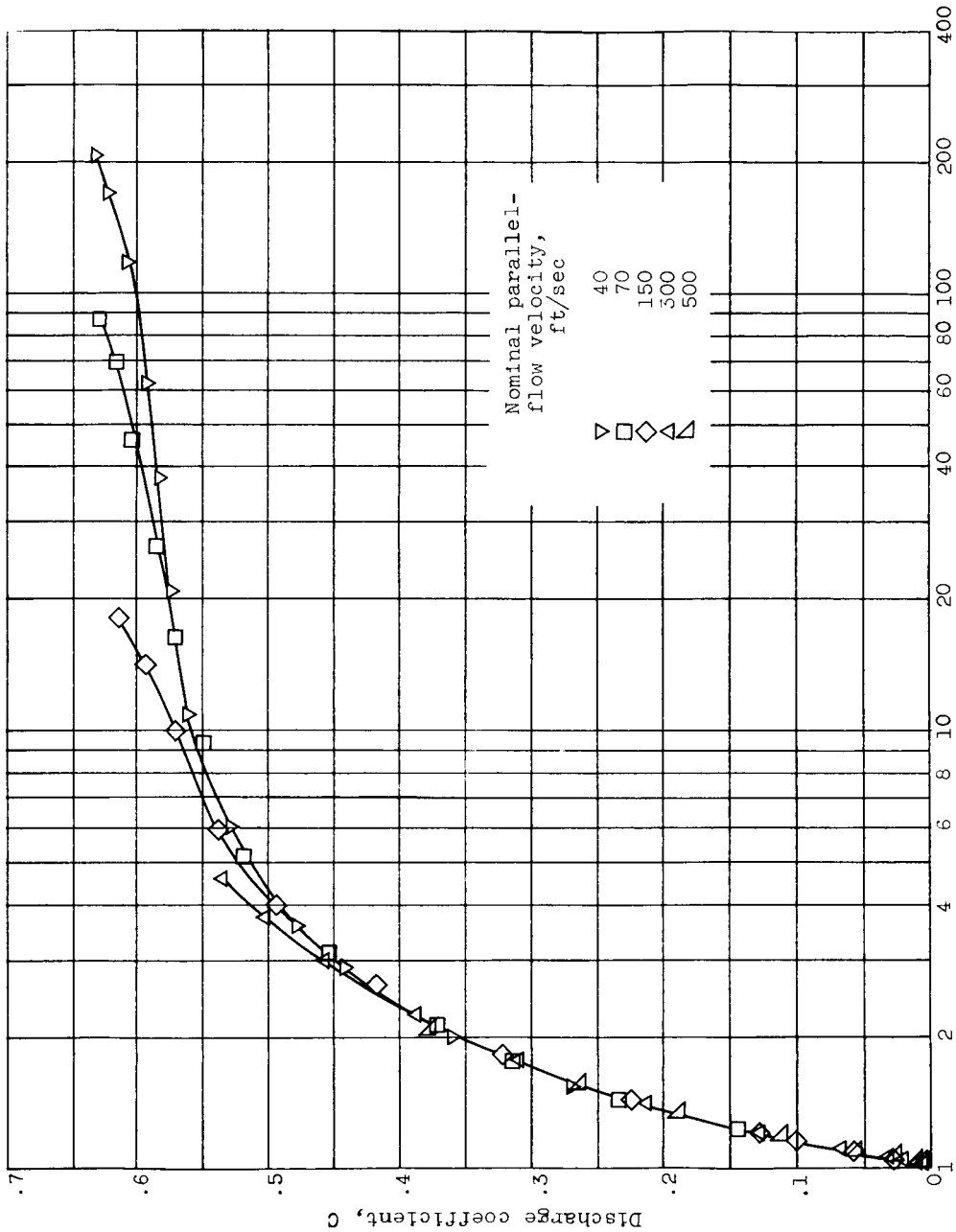

Figure 4. - Variation of hole discharge coefficient with flow parameter at various parallel-flow velocities. Hole diameter, 0.75 inch; wall thickness at hole, 0.040 inch.

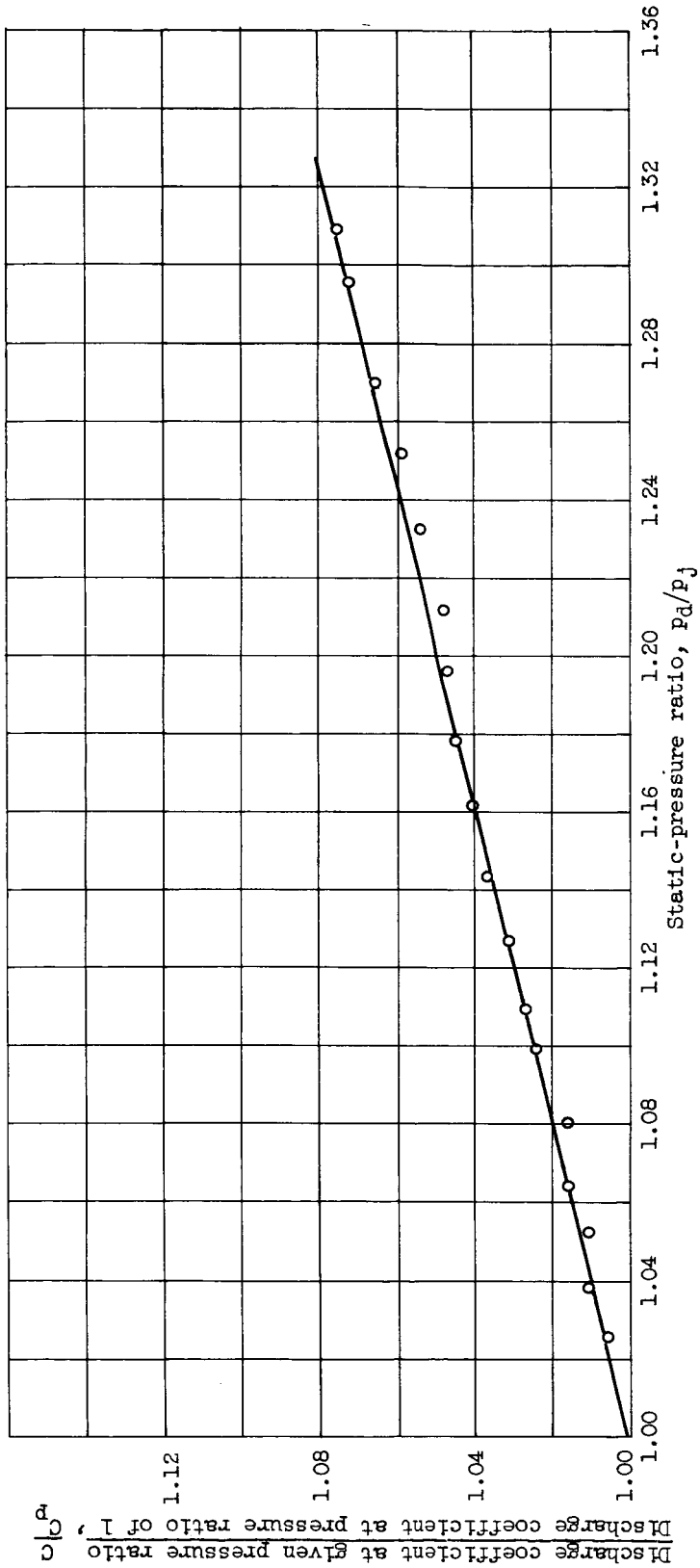

Figure 5. - Pressure-ratio correction factor for hole discharge coefficients (data from fig. 3). Hole diameter, 0.75 inch; wall thickness at hole, 0.040 inch.

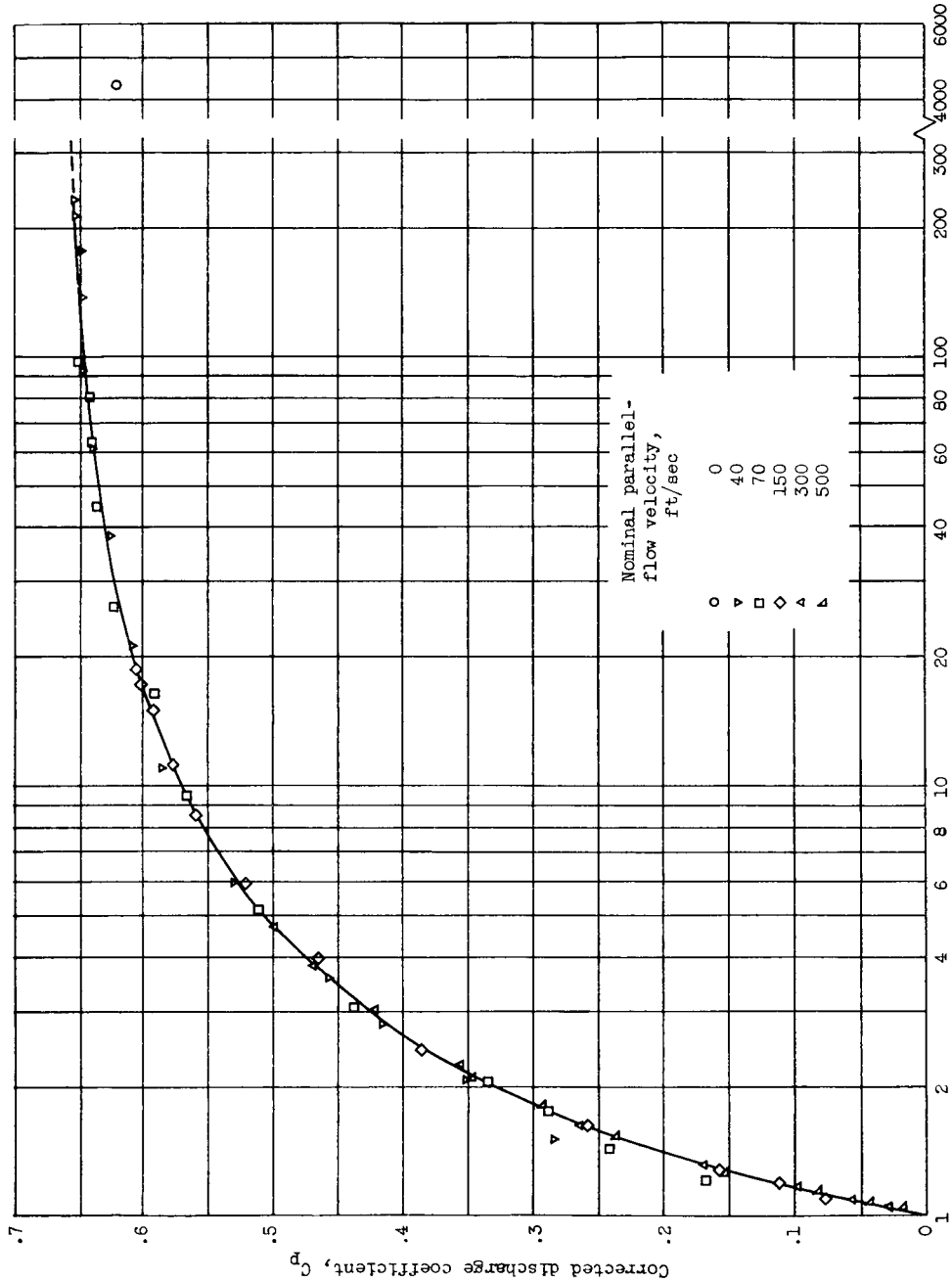

(a) Hole diameter, 0.125 inch; wall thickness at hole, 0.040 inch; duct height, 1.98 inches; duct static pressure, 1910 pounds per square foot absolute; boundary-layer thickness, 0.04 inch.

Figure 6. - Variation of corrected discharge coefficient with flow parameter.

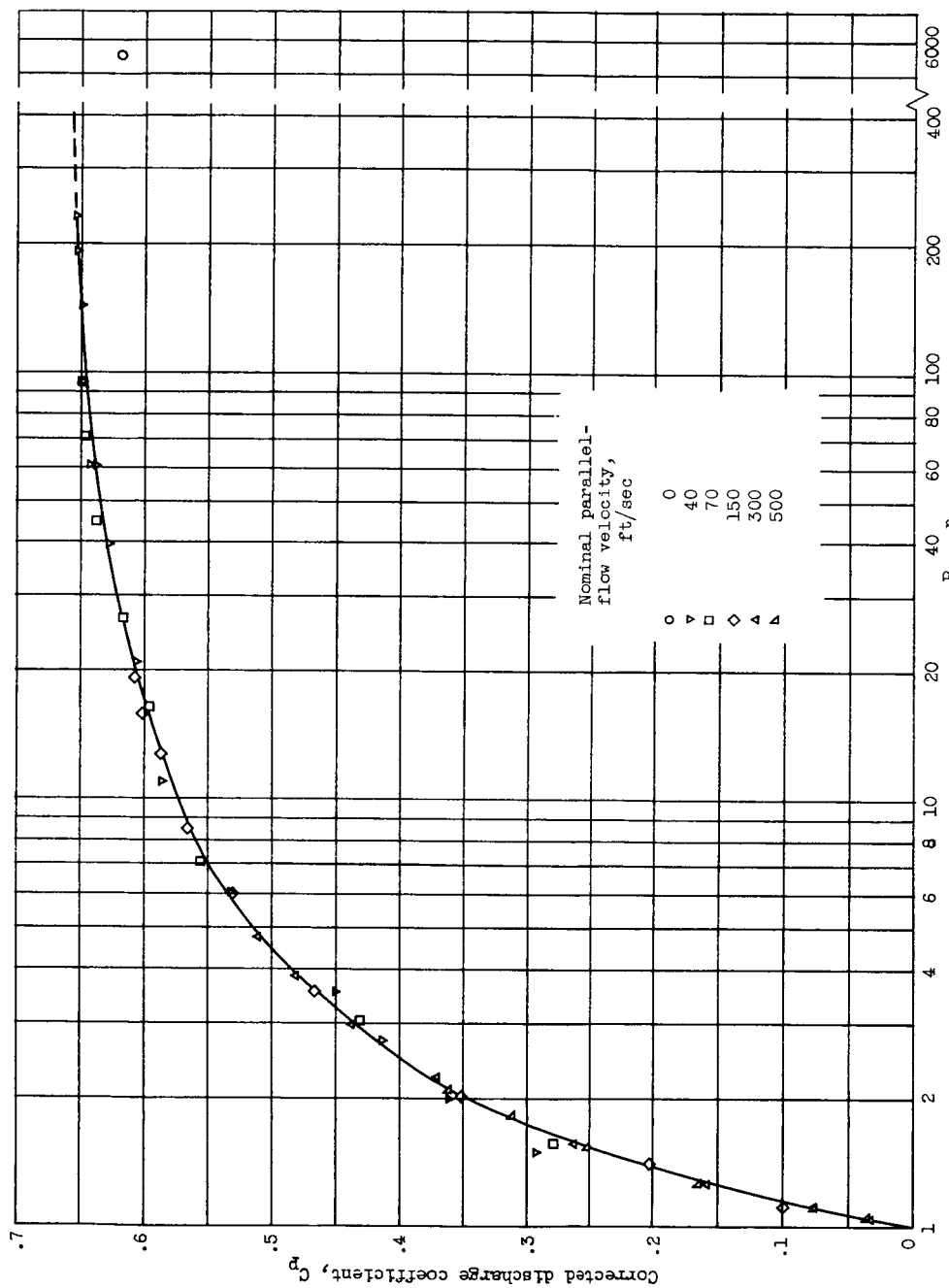

(b) Hole diameter, 0.125 inch; wall thickness at hole, 0.040 inch; duct height, 2.23 inches; duct static pressure, 1910 pounds per square foot absolute; boundary-layer thickness, 0.10 inch.

Figure 6. - Continued. Variation of corrected discharge coefficient with flow parameter.

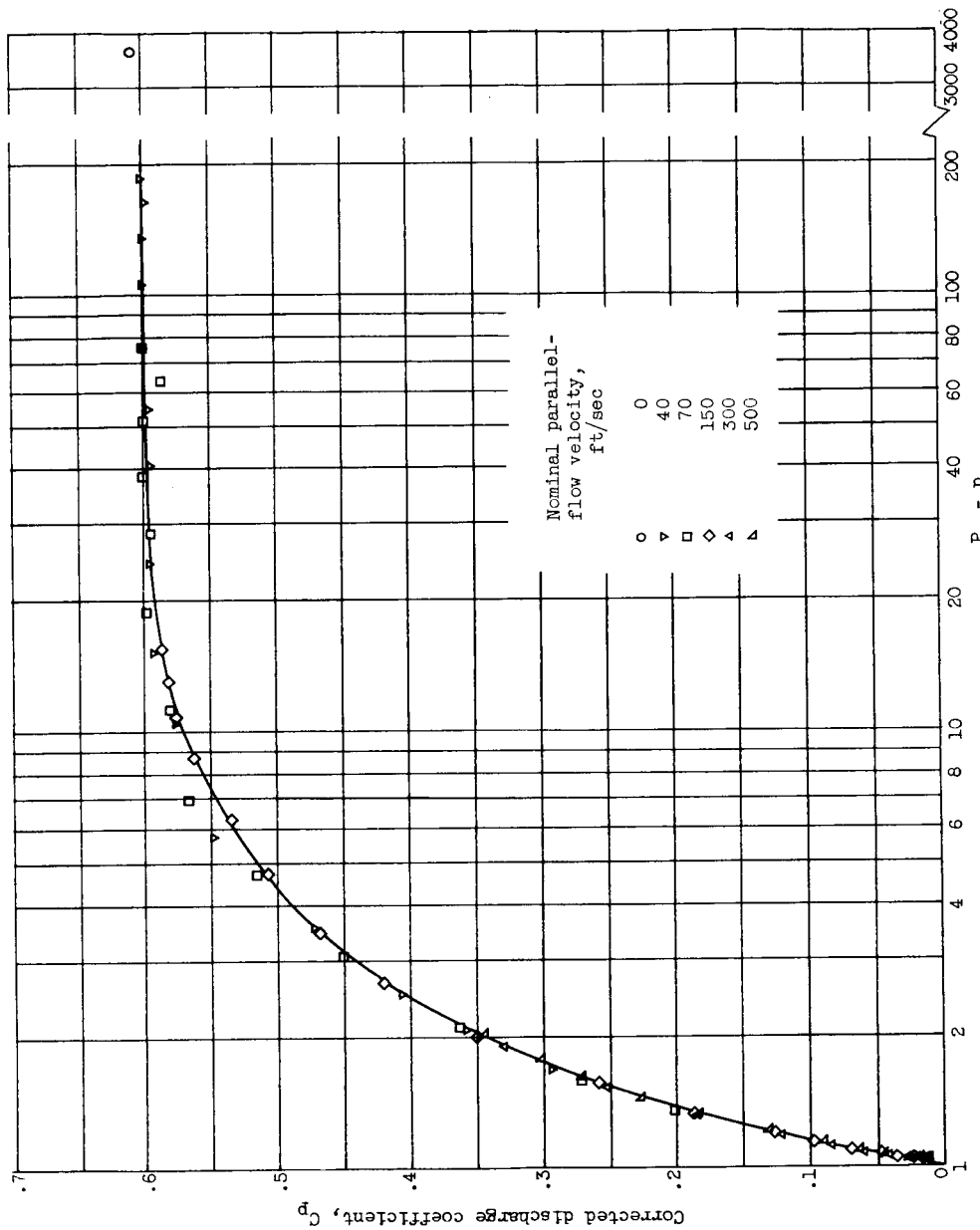

(c) Hole diameter, 0.250 inch; wall thickness at hole, 0.040 inch; duct height, 2.23 inches; duct static pressure, 1910 pounds per square foot absolute; boundary-layer thickness, 0.10 inch.

Figure 6. - Continued. Variation of corrected discharge coefficient with flow parameter.

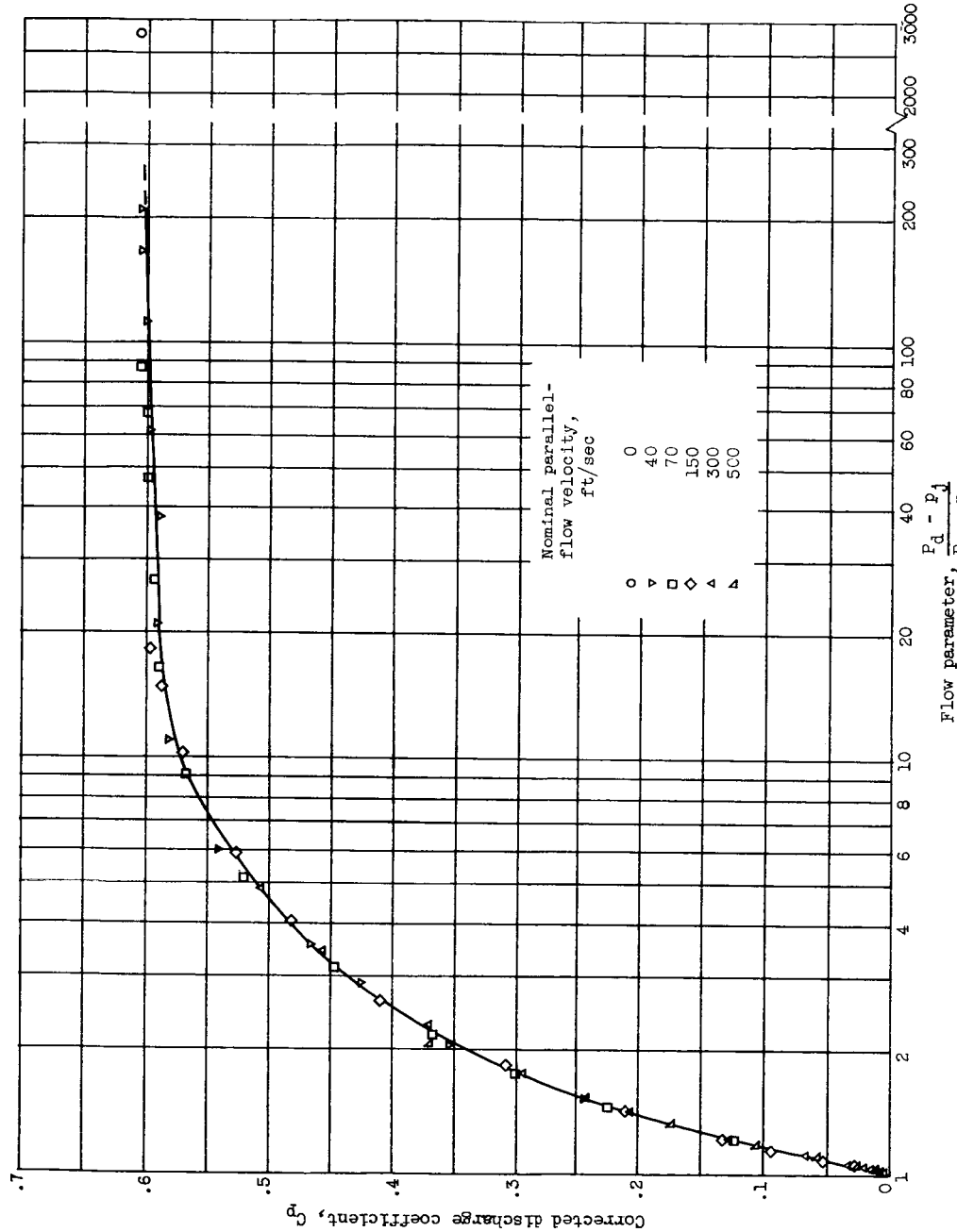

(d) Hole diameter, 0.250 inch; wall thickness at hole, 0.040 inch; duct height, 1.98 inches; duct static pressure, 1910 pounds per square foot absolute; boundary-layer thickness, 0.04 inch.

Figure 6. - Continued. Variation of corrected discharge coefficient with flow parameter.

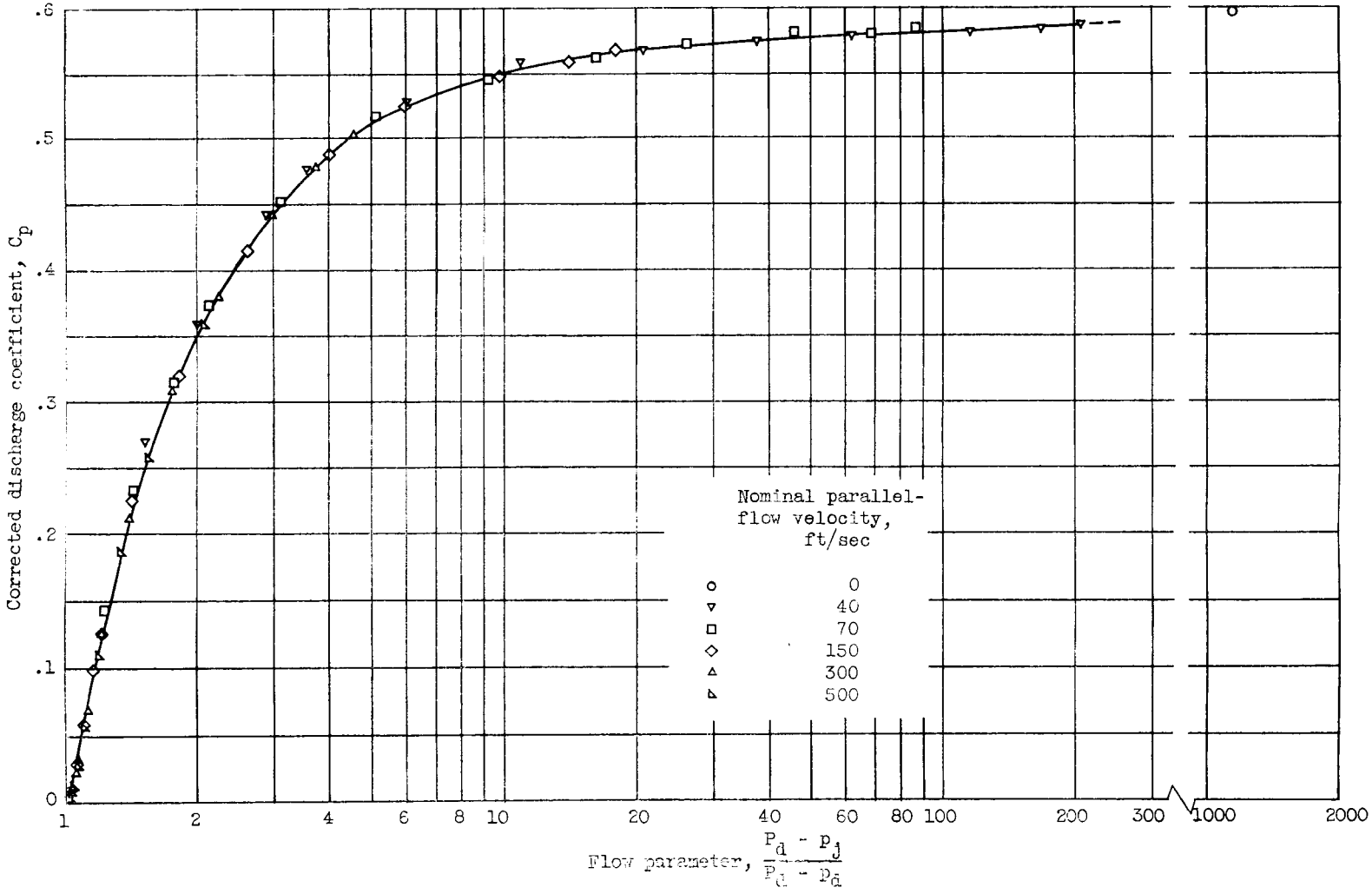

(a) Hole diameter, 0.760 inch; [illegible] hole, 0.040 inch; duct height, 2.23 inches; duct static pressure, [illegible] pounds per square [illegible]

Figure 6. - [illegible] parameter.

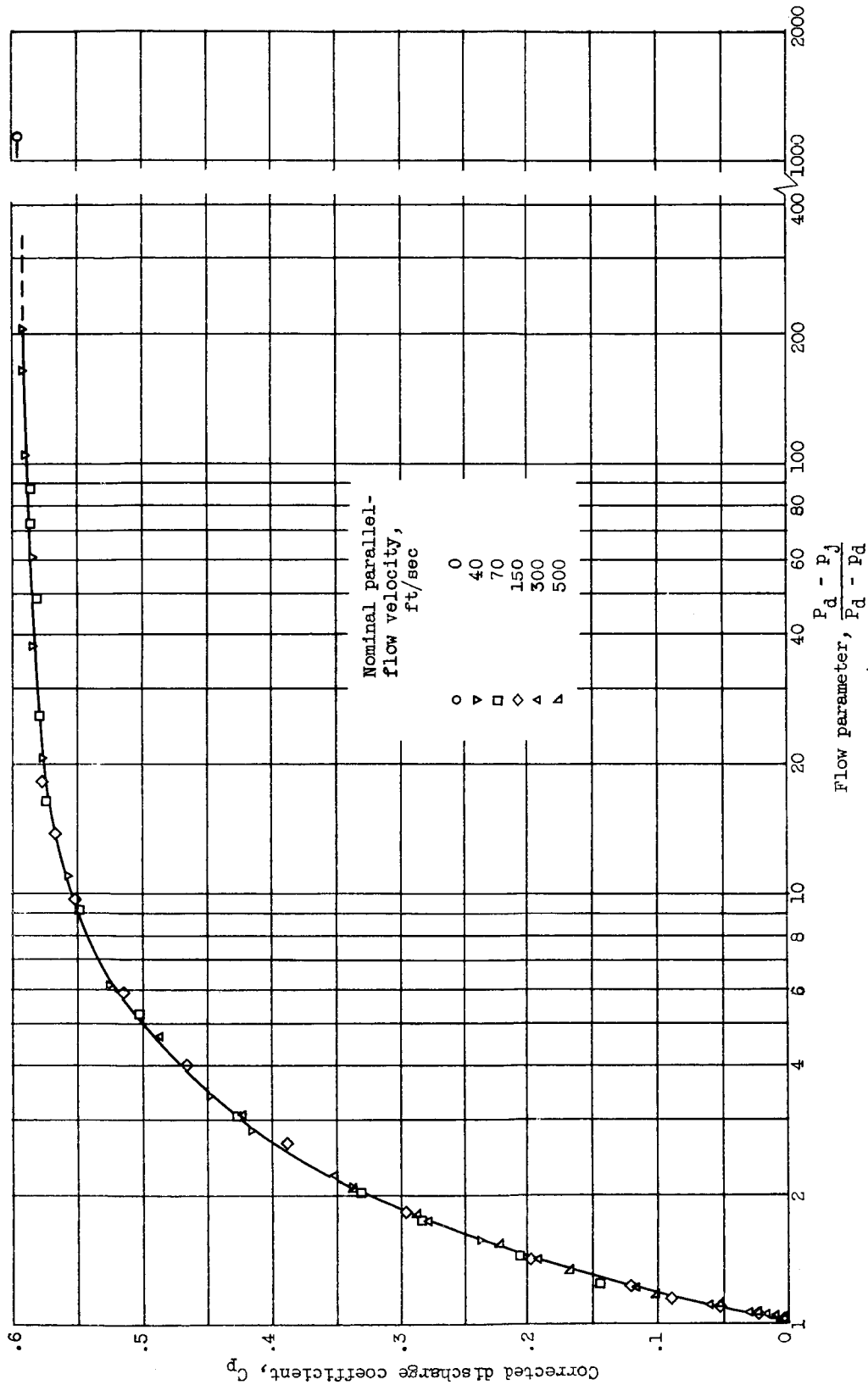

(f) Hole diameter, 0.750 inch; wall thickness at hole, 0.125 inch; duct height, 2.23 inches; duct static pressure, 1910 pounds per square foot absolute; boundary-layer thickness, 0.10 inch.

Figure 6. - Continued. Variation of corrected discharge coefficient with flow parameter.

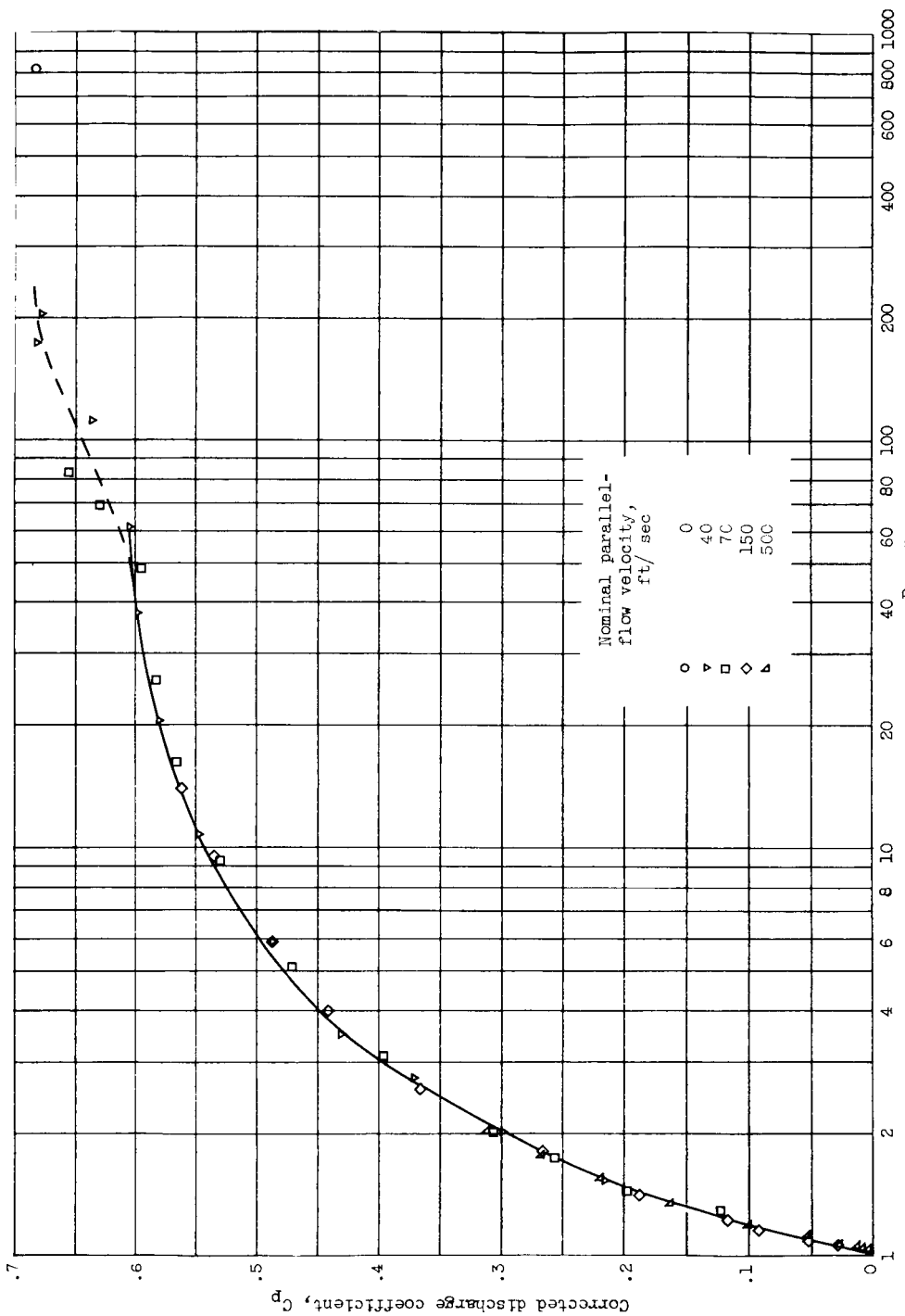

(g) Hole diameter, 0.750 inch; wall thickness at hole, 0.500 inch; duct height, 2.23 inches; duct static pressure, 1910 pounds per square foot absolute; boundary-layer thickness, 0.10 inch.

Figure 6. - Continued. Variation of corrected discharge coefficient with flow parameter.

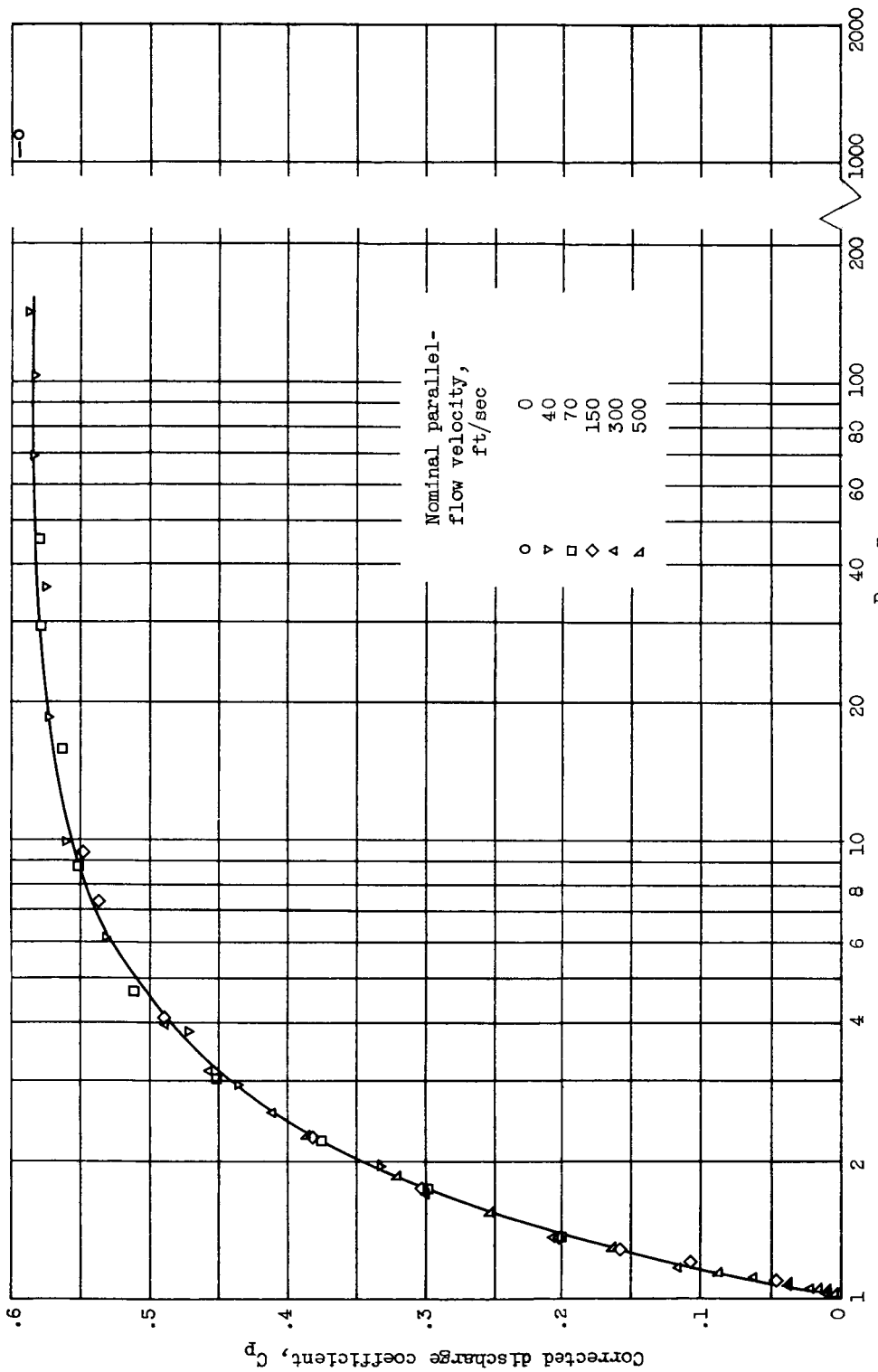

(h) Hole diameter, 0.750 inch; wall thickness at hole, 0.040 inch; duct height, 2.23 inches, duct static pressure, 1060 pounds per square foot absolute; boundary-layer thickness, 0.10 inch.

Figure 6. - Continued. Variation of corrected discharge coefficient with flow parameter.

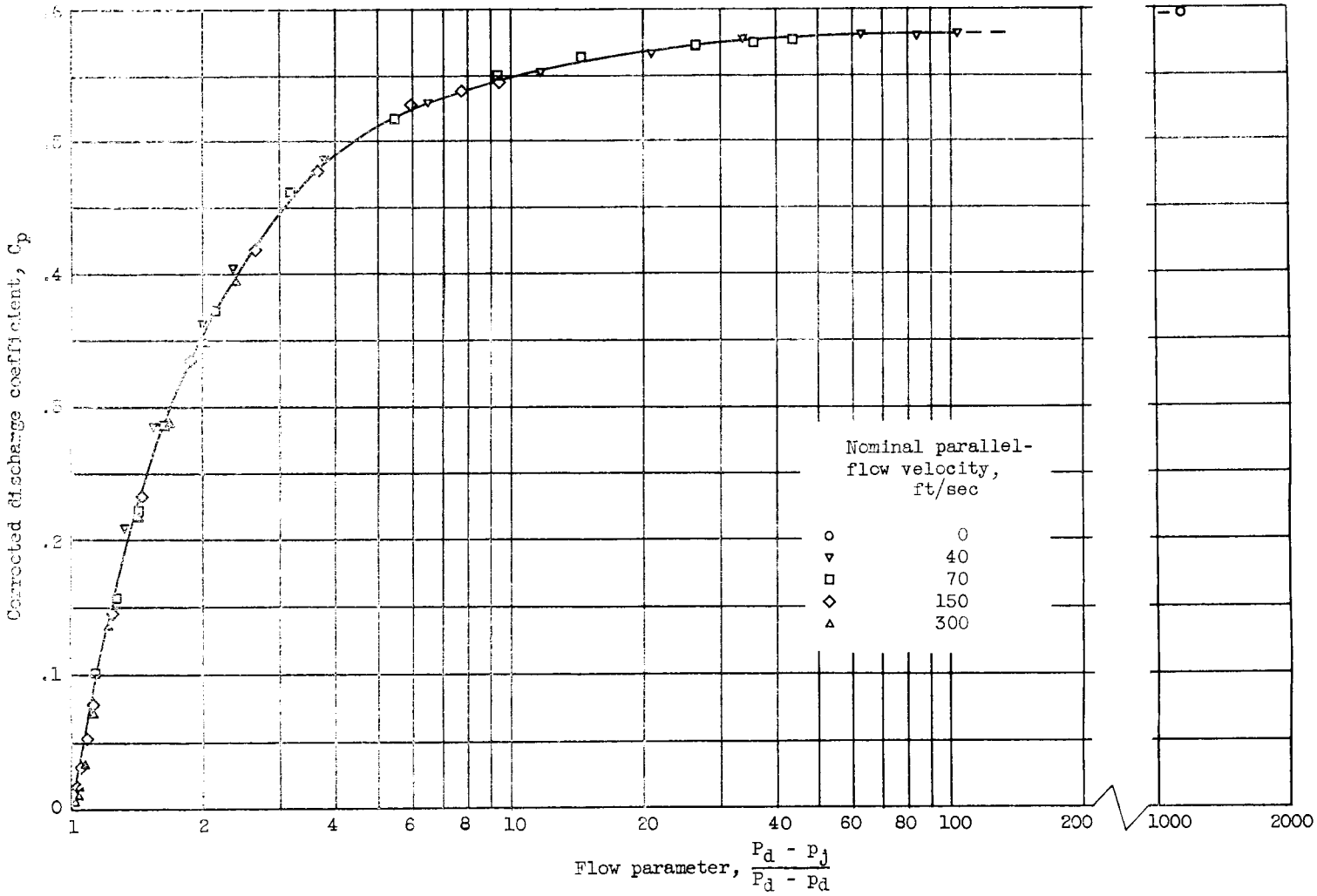

(i) Hole diameter, 0.750 inch; wall thickness at hole, 0.040 inch; duct height, 2.23 inches; duct static pressure, 3605 pounds per square foot absolute; boundary-layer thickness, 0.10 inch.

Figure 6. - Continued. Variation of corrected discharge coefficient with flow parameter.

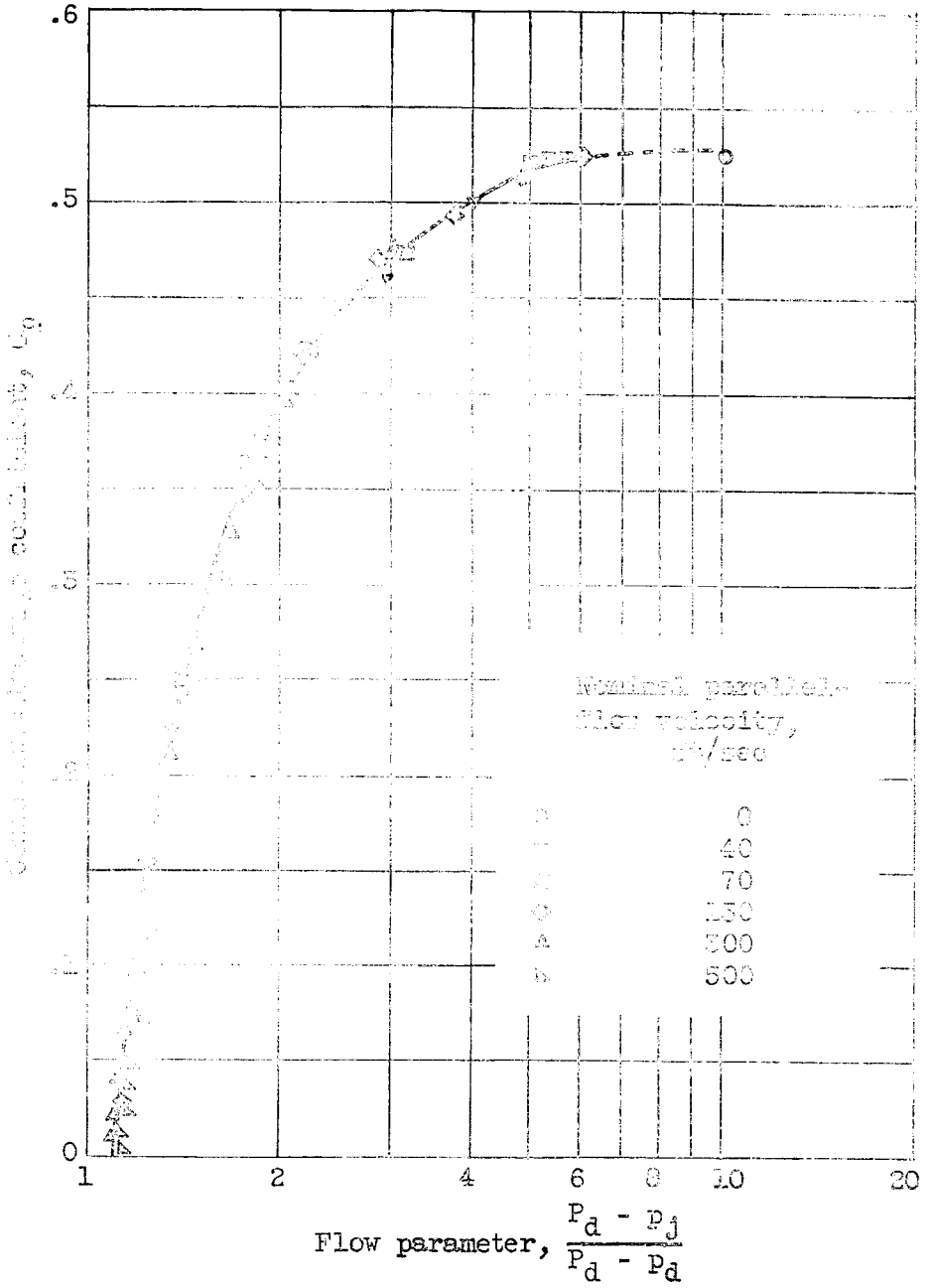

(j) Hole diameter, 1.50 inches; wall thickness at hole; 0.040 inch; duct height, 0.74 inch; duct static pressure, 1910 pounds per square foot absolute; boundary-layer thickness, 0.12 inch.

Figure 6. - Continued. Variation of corrected discharge coefficient with flow parameter.

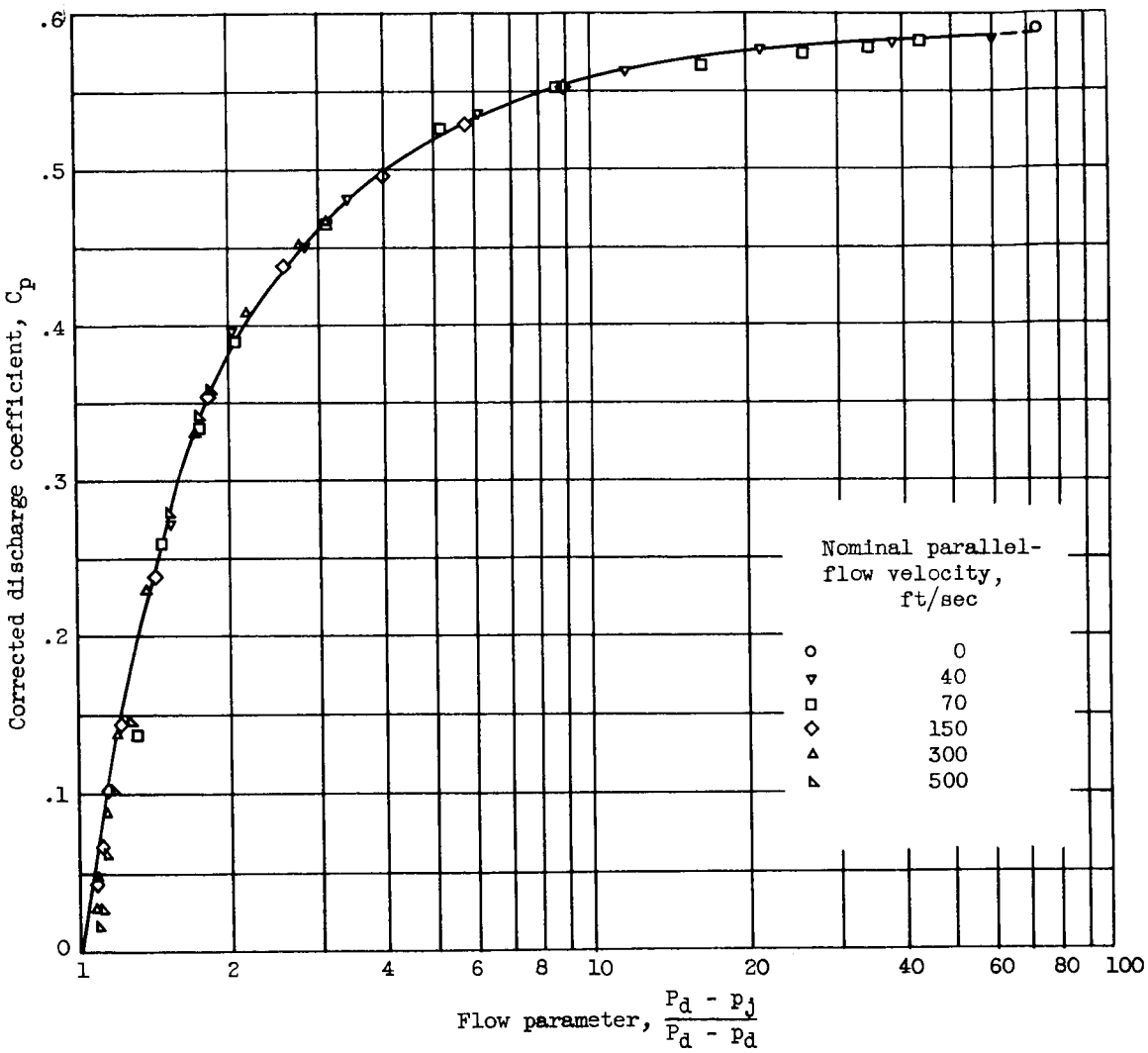

(k) Hole diameter, 1.50 inches; wall thickness at hole, 0.040 inch; duct height, 2.23 inches; duct static pressure, 1910 pounds per square foot absolute; boundary-layer thickness, 0.18 inch.

Figure 6. - Concluded. Variation of corrected discharge coefficient with flow parameter.

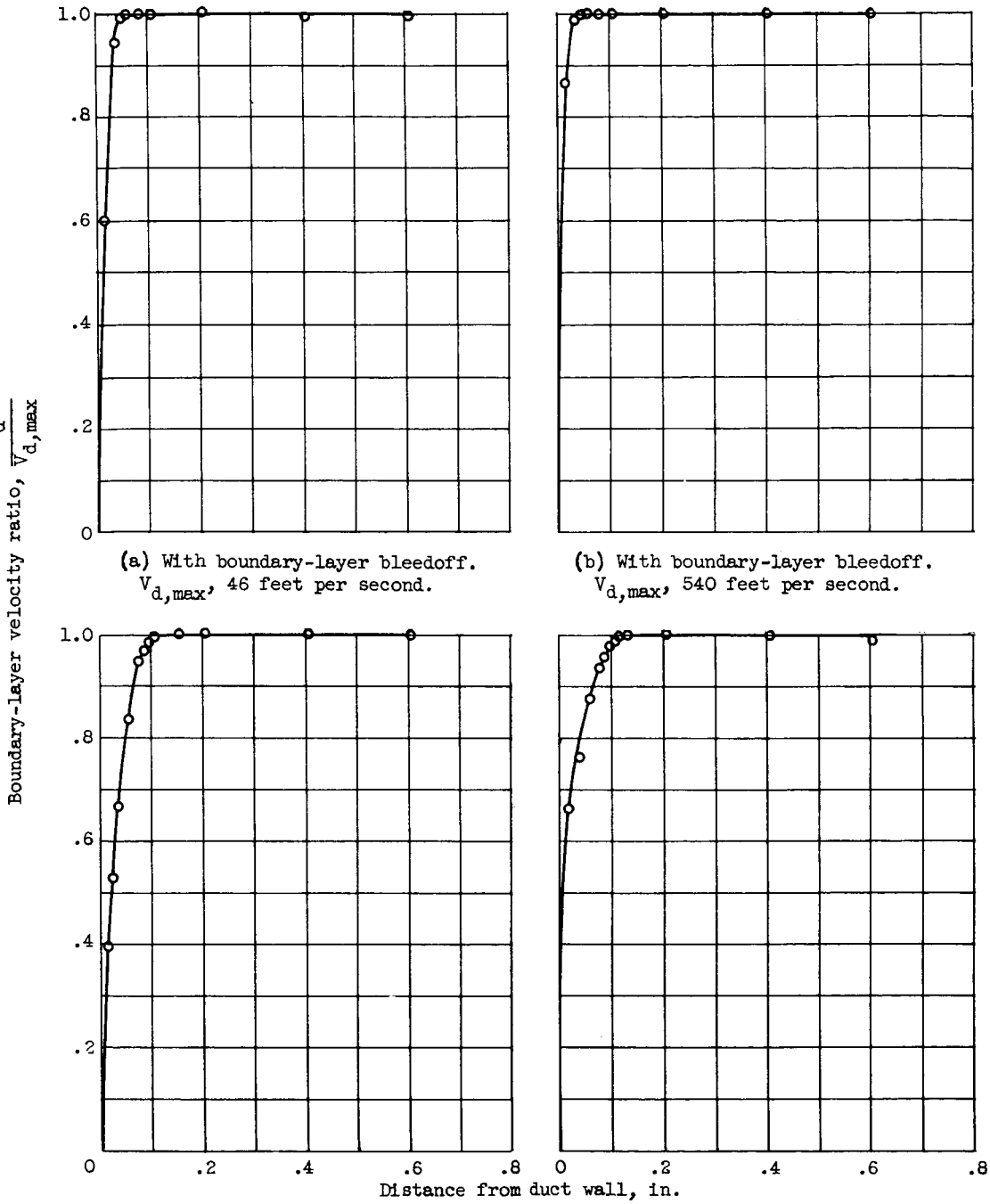

(a) With boundary-layer bleedoff. $V_{d,max}$, 46 feet per second.

(b) With boundary-layer bleedoff. $V_{d,max}$, 540 feet per second.

(c) Without boundary-layer bleedoff. $V_{d,max}$, 45 feet per second.

(d) Without boundary-layer bleedoff. $V_{d,max}$, 539 feet per second.

Figure 7. - Boundary-layer velocity profiles 1 inch upstream of center of test hole.

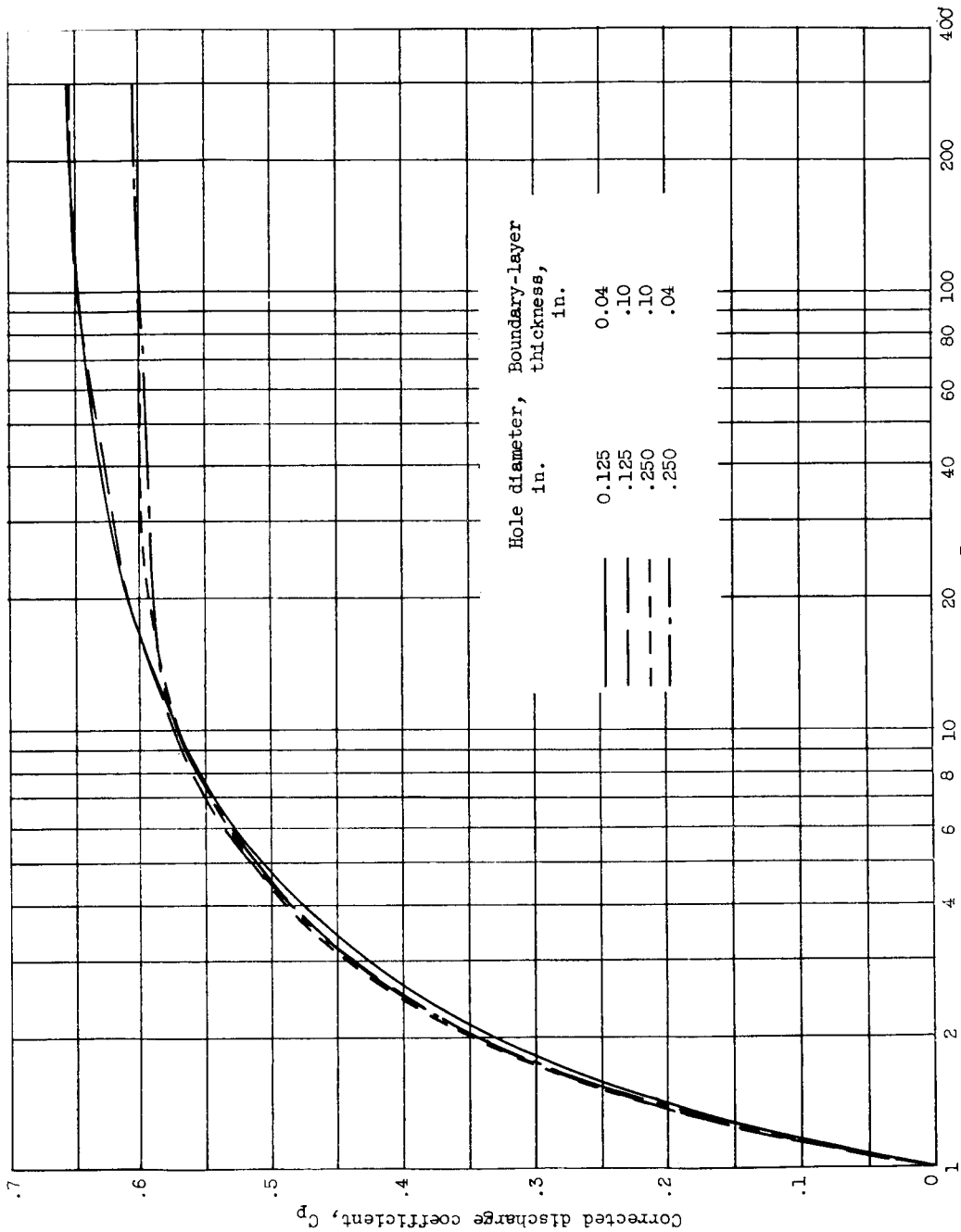

Figure 8. - Effect of boundary-layer thickness on corrected discharge coefficient of small holes.

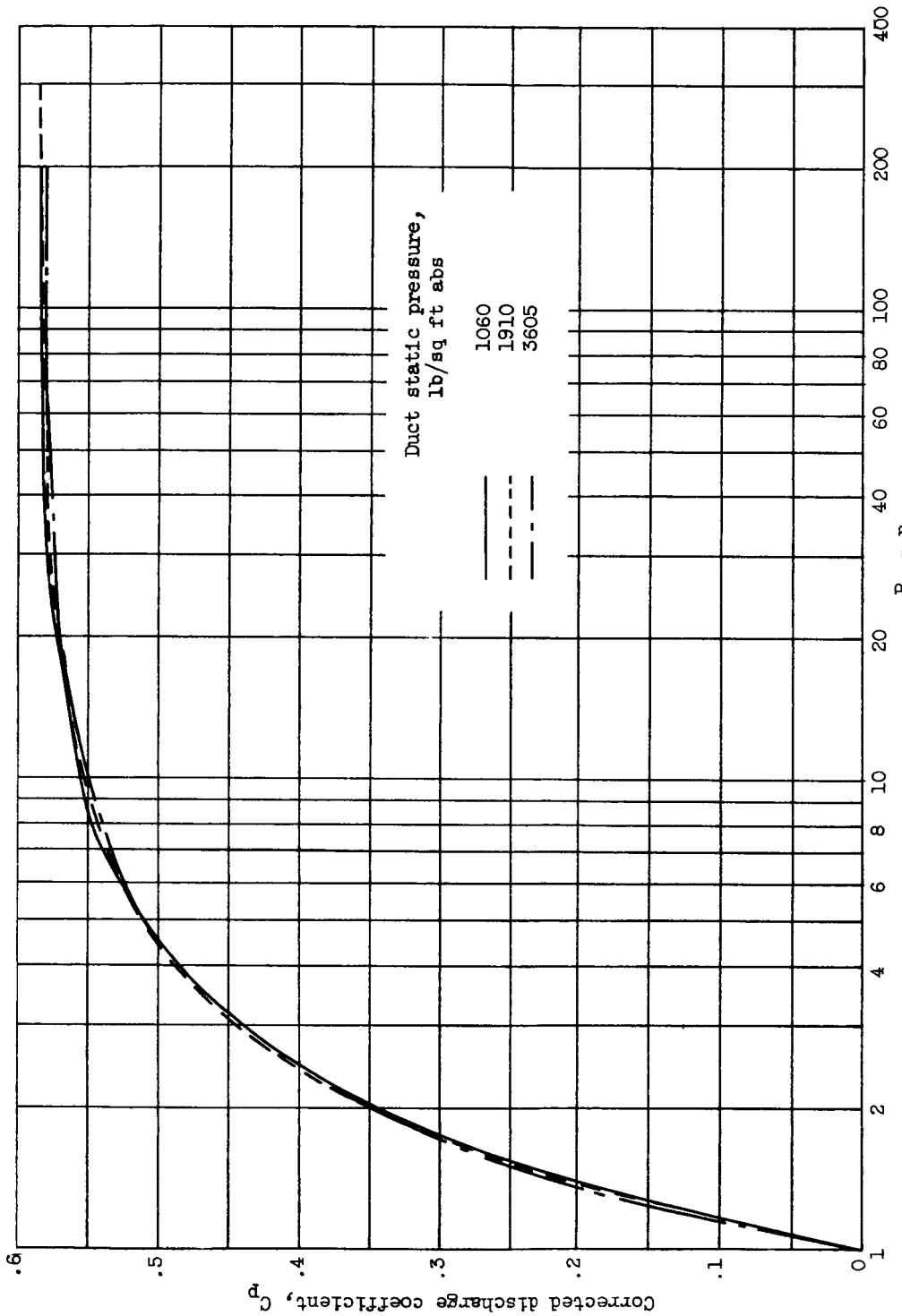

Figure 9. - Effect of duct static-pressure level on corrected discharge coefficient. Hole diameter, 0.75 inches.

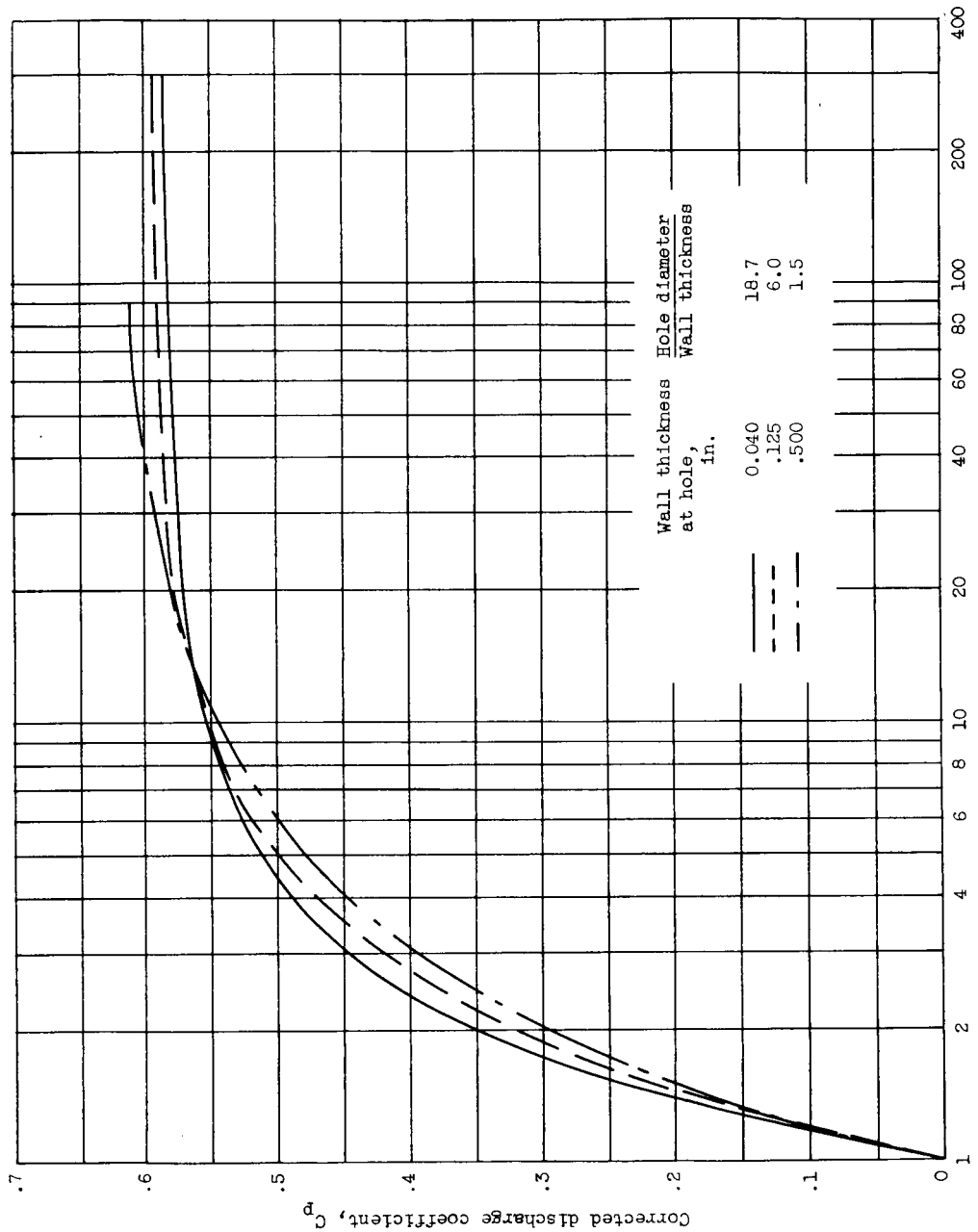

Figure 10. - Effect of wall thickness on corrected discharge coefficient. Hole diameter, 0.750 inch.

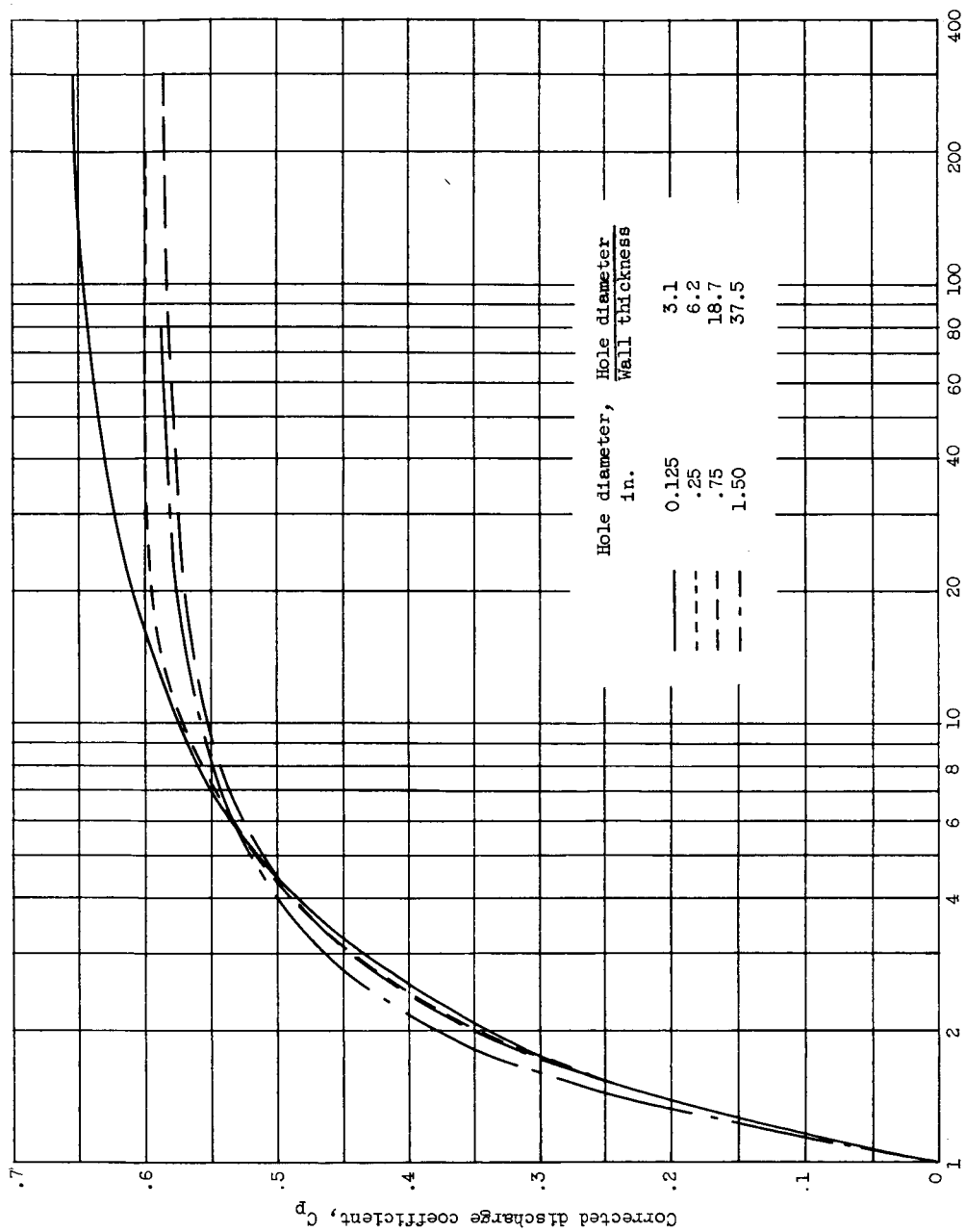

Figure 11. - Effect of hole diameter on corrected discharge coefficient. Wall thickness at hole, 0.040 inch.

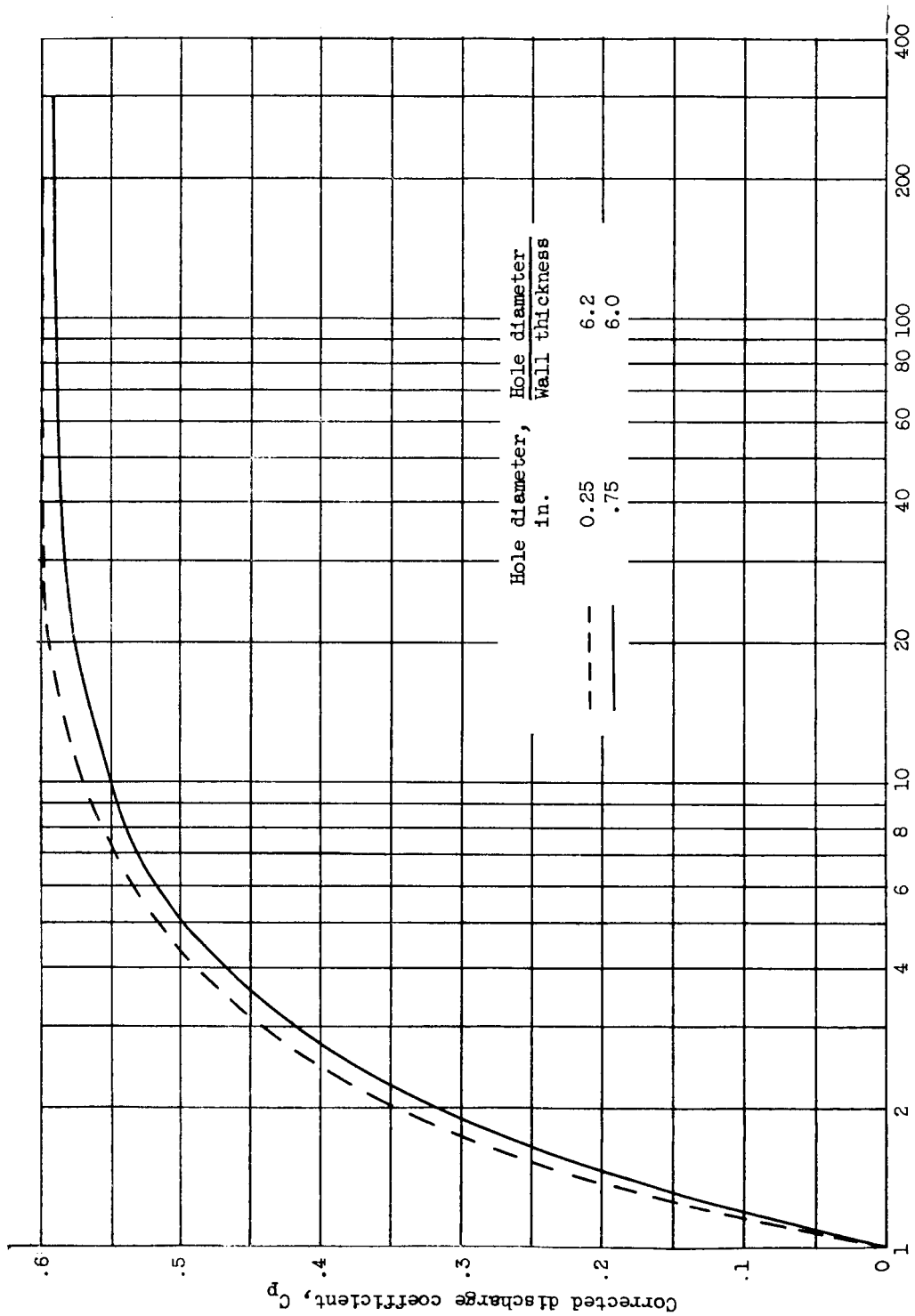

Figure 12. - Comparison of corrected discharge coefficients of holes with different diameters having constant ratio of hole diameter to wall thickness.

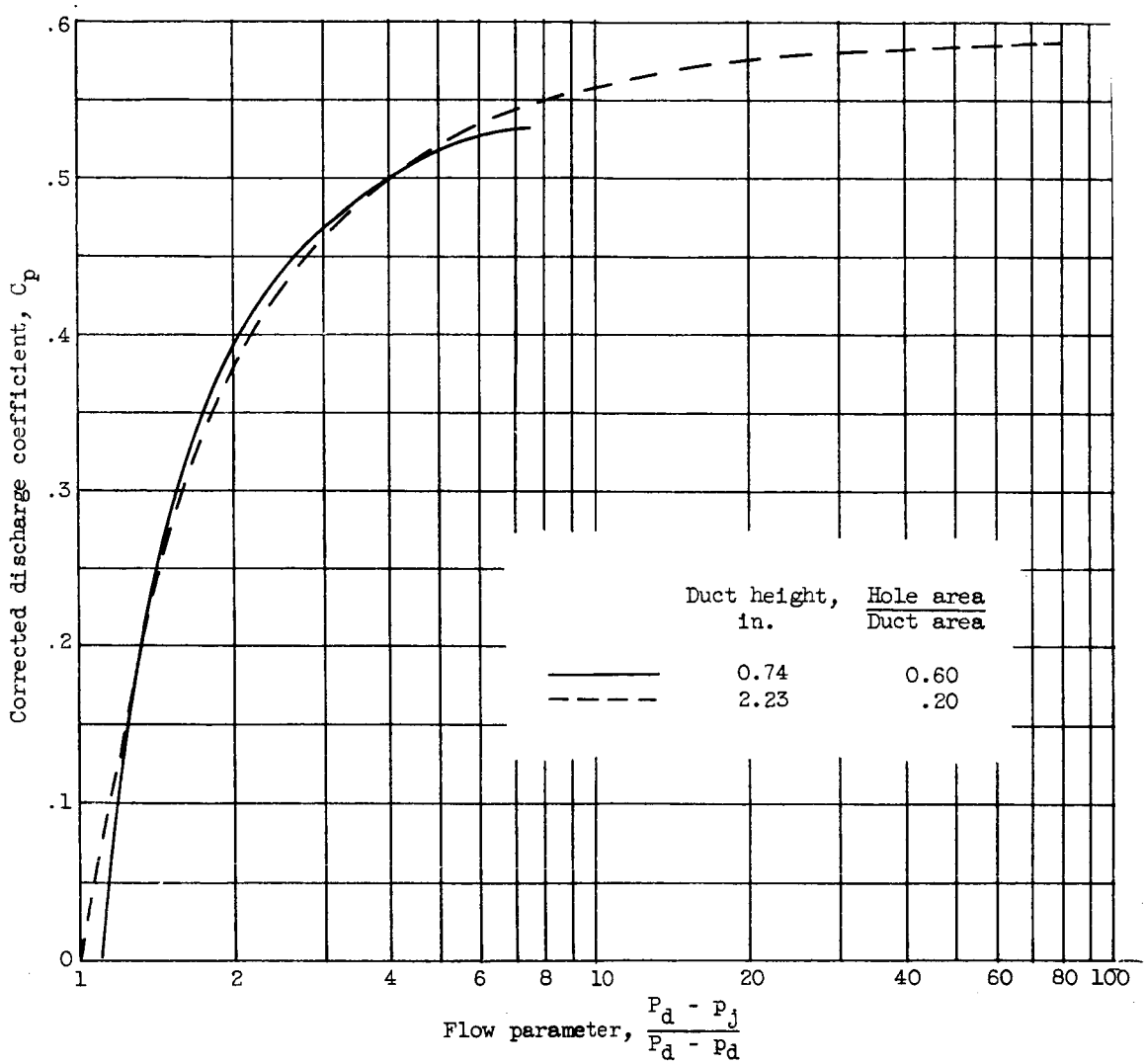

Figure 13. - Effect of parallel-flow duct height on corrected discharge coefficient. Hole diameter, 1.50 inches, duct width, 4.0 inches.